

Cross-ratio dynamics and the dimer cluster integrable system

Niklas Affolter

Terrence George

Sanjay Ramassamy

August 31, 2021

Abstract

Cross-ratio dynamics, allowing to construct 2D discrete conformal maps from 1D initial data, is a well-known discrete integrable system in discrete differential geometry. We relate it to the dimer integrable system from statistical mechanics by identifying its invariant Poisson structure and integrals of motion recently found by Arnold et al. to the Goncharov-Kenyon counterparts for the dimer model on a specific class of graphs. This solves the open question of finding a cluster algebra structure describing cross-ratio dynamics. The main tool relating geometry to the dimer model is the definition of triple crossing diagram maps associated to bipartite graphs on the cylinder. In passing we write the bivariate polynomial defining the dimer spectral curve for arbitrary bipartite graphs on the torus as the characteristic polynomial of a one-parameter family of matrices, a result which may be of independent interest.

1 Introduction

Consider maps $f : \mathbb{Z}^2 \rightarrow \mathbb{CP}^1$ such that

$$\frac{(f_{i,j} - f_{i+1,j})(f_{i+1,j+1} - f_{i,j+1})}{(f_{i+1,j} - f_{i+1,j+1})(f_{i,j+1} - f_{i,j})} = \alpha_j, \quad (1)$$

where $\alpha_j \in \mathbb{C} \setminus \{0\}$ and all $i, j \in \mathbb{Z}$. Such a map is a special case of a discrete version of the Schwarzian KdV equation [NC95], or a special case of a *discrete isothermic surface* [BP96] restricted to the sphere S^2 . In both cases it was shown that these maps are a discrete integrable system in the sense that they admit a discrete Lax representation. An interesting question is: Given all α_j , what is the space of solutions of (1)? To answer this, consider each column i of \mathbb{Z}^2 as a discrete curve $f_i : \mathbb{Z} \rightarrow \mathbb{CP}^1$. The discrete curves corresponding to two adjacent columns f_i and f_{i+1} are called $\vec{\alpha}$ -related, where $\vec{\alpha}$ is the vector of all α_j . In the case when α_j is independent of j , the curve f_{i+1} is called a *Darboux transform* [HJ03] of f_i in the discrete differential geometry community. If we know f_i and one point of f_{i+1} , then equation (1) determines all of f_{i+1} . As a consequence, there is a complex one parameter freedom for each additional column of \mathbb{Z}^2 . However, this changes if one considers *periodic* maps, that is maps $\mathbb{Z} \times \mathbb{Z}/m\mathbb{Z} \rightarrow \mathbb{CP}^1$ for some $m \in \mathbb{N}$ that satisfy equation (1). In this case, if we know f_i then there are only two possible solutions for f_{i+1} , because f_{i+1} has to be periodic as well. Thus if we know both f_{i-1} as well as f_i and assume that $f_{i+1} \neq f_{i-1}$, then f_{i+1} is determined *uniquely*. Special attention has been paid to the case that α_j does not depend on j . In this case, periodic solutions to equation (1) have been studied as *periodic discrete conformal maps* [HJMNP01] with respect to algebro-geometric integrability. Also in this case, the map $(f_{i-1}, f_i) \mapsto (f_i, f_{i+1})$ is called *cross-ratio dynamics* [AFIT20]. Cross-ratio dynamics can also

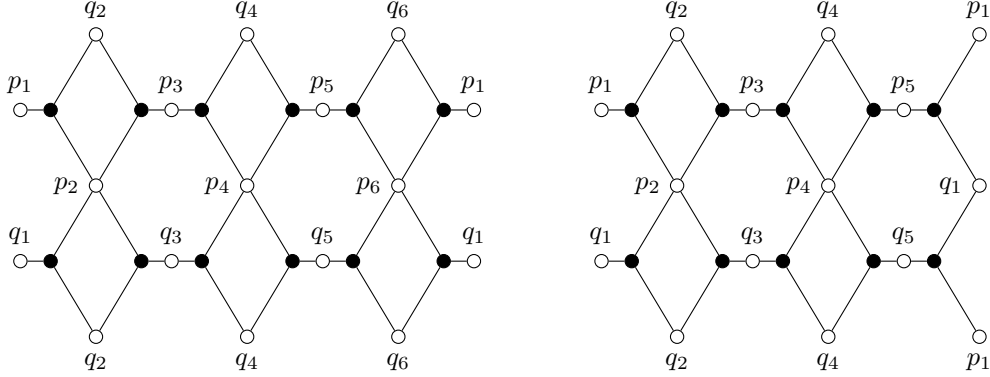


Figure 1: The relevant bipartite graphs to describe a pair of curves of length $n = 6$ (left) and length $n = 5$ (right). Here the top and the bottom sides of each graph are identified, yielding the cylinder graphs $\Gamma_{6,\mathbb{A}}$ and $\Gamma_{5,\mathbb{A}}$. If we additionally identify the left and right sides of each graph, we obtain the torus graphs Γ_6 and Γ_5 .

be generalized from discrete periodic curves to discrete *twisted* curves, that is curves $f_i : \mathbb{Z} \rightarrow \mathbb{CP}^1$ such that $f_i(j+n) = M \circ f_i(j)$ for all $j \in \mathbb{Z}$ and for some $n \in \mathbb{N}$ and $M \in \text{PGL}_2$. For cross-ratio dynamics the integrability in the sense of Liouville was proved by Arnold, Fuchs, Izmistiev and Tabachnikov [AFIT20]. Indeed, they provide Poisson brackets that are preserved by the dynamics as well as integrals of motion that are Casimirs and Hamiltonians. We will henceforth call them the AFIT Poisson structures, Casimirs and Hamiltonians.

Another widely studied discrete system which is integrable both in the algebro-geometric sense and in the Liouville sense is the dimer model on bipartite graphs on the torus [GK13] coming from statistical mechanics. Goncharov and Kenyon identified a Poisson structure on the space of face weights associated to a given graph and obtained the Casimirs and Hamiltonians of the underlying integrable system as coefficients of the polynomial defining the spectral curve of the model. Our first main result consists in identifying the AFIT Liouville integrable structure [AFIT20] with the Goncharov-Kenyon Liouville integrable structure [GK13] for a special class of graphs. It is stated loosely in Theorem 1.1 below and stated in full detail as Theorem 6.7 and Theorem 7.1 later. Let G (resp. G^{odd}) be the cylinder graph represented on the left (resp. right) of Figure 8. In both pictures, the top and the bottom sides of the rectangle are identified. If n is even, let Γ_n be the torus graph obtained by gluing in a cyclic chain $\frac{n}{2}$ copies of G . If n is odd let Γ_n be the torus graph obtained by gluing in a cyclic chain $\frac{n-1}{2}$ copies of G and one copy of G^{odd} . See Figure 1 for pictures of Γ_6 and Γ_5 . In this article we consider a more general setup than [AFIT20], namely we assume that the α_j are periodic of period n , but not necessarily constant.

Theorem 1.1. *Let $n \geq 2$. The AFIT Poisson structure, Casimirs and Hamiltonians for cross-ratios dynamics for twisted discrete curves coincide with the Goncharov-Kenyon Poisson structure, Casimirs and Hamiltonians for the dimer integrable system on the torus graph Γ_n .*

In order to prove Theorem 1.1, we find an expression for the bivariate polynomial defining the dimer spectral curve for general bipartite graphs on the torus as the characteristic polynomial of a matrix depending on a single parameter. More precisely, given an edge-weighted bipartite graph

Γ on the torus, we construct a matrix $\Pi(w)$ depending on a parameter w and on the choice of a zigzag path in Γ . Then we have

Theorem 1.2. *The spectral curve of the dimer model on Γ is given by*

$$\{(z, w) \in (\mathbb{C}^*)^2, \det(zI - \Pi(w)) = 0\}$$

Theorem 1.2 holds for general graphs and not just for those related to cross-ratio dynamics, hence it may be of independent interest. The matrix $\Pi(w)$ is reminiscent of the boundary measurement matrix for networks on cylinders of [GSV12, GSTV16]. In a recent preprint of which we learned during the completion of this work, Izosimov [Izo21] made precise the connection between the integrable systems of [GK13] and [GSTV16]. In particular his main result provides a representation of the dimer spectral curve similar to Theorem 1.2. We note that analogous representations have appeared in physics in the special case of the periodic Toda chain [EFS12] and in mathematical physics via representation-theoretic arguments [FM16].

Theorem 1.1 realizes cross-ratio dynamics as a special case of the dimer integrable system by adopting an analytic point of view using coordinates on the spaces on which the two dynamics occur. One can actually provide a more geometric identification by making use of the recently introduced [AGR] triple crossing diagram maps (TCD maps). These maps, a version of the vector-relation configurations of [AGPR19] better adapted to geometric dynamics, associate a geometric configuration in some projective space $\mathbb{C}P^m$ to a bipartite graph on a disk with trivalent black vertices. To each white vertex is associated a point in $\mathbb{C}P^m$, with the constraint that any three points associated to the neighbors of a black vertex must be aligned. One can perform local changes of the geometric configuration of a TCD map which are associated with the dimer local moves for bipartite graphs. Using appropriate coordinates, these moves carry an interpretation in terms of cluster algebra mutations.

In this article, we introduce the notion of twisted TCD maps on the cylinder. Let $\Gamma_{n,\mathbb{A}}$ be the cylinder graph obtained by gluing together the same cylinder graphs as for Γ_n but without closing up cyclically (see Figure 1 for two examples). An explicit bridge between cross-ratio dynamics and the dimer model is given by the following result:

Theorem 1.3. *Pairs of $\vec{\alpha}$ -related twisted discrete curves arise as twisted TCD maps on $\Gamma_{n,\mathbb{A}}$ and cross-ratio dynamics arises as an explicit sequence of local moves on these twisted TCD maps.*

An important note regarding Theorem 1.3 is that the first local move in the sequence depends on a parameter and that parameter depends globally on the initial pair of $\vec{\alpha}$ -related twisted discrete curves. Furthermore, combining Theorem 1.1 with Theorem 1.3, we obtain an alternative proof of the conservation of the AFIT Hamiltonians, since the dynamics on TCD maps is conjugated to the dimer integrable dynamics of [GK13]. A more explicit statement of Theorem 1.3 is given by Theorem 8.2. As a corollary, we answer an open question of [AFIT20] asking for an interpretation of cross-ratio dynamics in terms of cluster algebras. Indeed, all but the first and the last operations for TCD maps of Theorem 1.3 has a cluster algebra interpretation [AGPR19, AGR].

Corollary 1.4. *The evolution of the some coordinates under cross-ratio dynamics can be written as an explicit composition of operations, with all but the first and the last one being cluster algebra mutations.*

Here we mean mutations of cluster variables known as y [FZ02] or as X [FG09] depending on the authors.

As noted by [AFIT20], cross-ratio dynamics bears a lot of resemblances with the pentagram map, another dynamical system on discrete curves for which several similar properties are known: Liouville integrability [OST10, OST13], algebro-geometric integrability [Sol13], cluster algebra interpretation [Gli11], dimer model interpretation [FM16, GR17] and realization in terms of TCD maps [AGPR19, AGR]. Similar properties are known or expected to hold for many generalizations of the pentagram map, see e.g. [GP16].

There is however a notable difference with cross-ratio dynamics. For the pentagram map and its generalizations, the dynamics is local in the sense that one can construct a point of the curve f_{i+1} knowing only a bounded number of points of the curve f_i . For cross-ratio dynamics the dynamics is global, one needs to know all the points of the curve f_i to construct any given point of f_{i+1} . This is related to the R-matrix constructions of [ILP16, ILP19, Che20].

Organization of the paper

In Section 2 we provide the necessary background on cross-ratio dynamics and its integrability following mostly [AFIT20], but generalizing to n -periodic \vec{a} . In Section 3 we recall the Goncharov-Kenyon integrable system [GK13] associated with the dimer model on the torus. In Section 4 we consider the dimer model on the cylinder, construct the matrix $\Pi(w)$ and prove Theorem 1.2. We introduce in Section 5 the notion of twisted TCD maps associated to a bipartite graph on the cylinder and use it in Section 6 to prove Theorem 1.1 when n is even. In Section 7 we explain how to modify the computations to derive this result when n is odd. Section 8 describes the sequence of local moves for twisted TCD maps that realize cross-dynamics, as stated in Theorem 1.3. Finally Appendix A presents some results used in Section 4 related to the classical Schur complement.

2 The cross-ratio dynamics integrable system

2.1 Multi-ratios

Given points $a_1, \dots, a_{2m} \in \mathbb{CP}^1$, let $\tilde{a}_1, \dots, \tilde{a}_{2m}$ denote a choice of lifts to \mathbb{C}^2 . Their *multi-ratio* is defined as

$$\text{mr}(a_1, a_2, \dots, a_{2m}) = \prod_{i=1}^m \frac{\det(\tilde{a}_{2i-1}, \tilde{a}_{2i})}{\det(\tilde{a}_{2i}, \tilde{a}_{2i+1})}, \quad (2)$$

where $\det(a, b)$ denotes the determinant of the matrix with columns $a, b \in \mathbb{C}^2$ and indices are taken modulo $2m$. When $m = 2$, the multi-ratio specializes to the *cross-ratio*

$$\text{cr}(a_1, a_2, a_3, a_4) = \frac{\det(\tilde{a}_1, \tilde{a}_2) \det(\tilde{a}_3, \tilde{a}_4)}{\det(\tilde{a}_2, \tilde{a}_3) \det(\tilde{a}_4, \tilde{a}_1)}. \quad (3)$$

The multi-ratio is PGL_2 invariant. If the points a_i are all in an affine chart $\mathbb{C} \subset \mathbb{CP}^1$, then we can choose lifts of the form $\tilde{a}_i = \begin{bmatrix} a_i \\ 1 \end{bmatrix}$, and then we have

$$\text{mr}(a_1, a_2, \dots, a_{2m}) = \prod_{i=1}^m \frac{a_{2i-1} - a_{2i}}{a_{2i} - a_{2i+1}}. \quad (4)$$

2.2 Discrete projective curves in \mathbb{CP}^1

A *discrete curve* is a map $p : \mathbb{Z} \rightarrow \mathbb{CP}^1$. A *twisted discrete curve* of length n is a pair (p, M) where $p : \mathbb{Z} \rightarrow \mathbb{CP}^1$ is a discrete curve and $M \in \mathrm{PGL}_2$ is a projective transformation called *monodromy* such that $p_{i+n} = M(p_i)$ for all $i \in \mathbb{Z}$. A twisted discrete curve (p, M) is *nondegenerate* if for all $i \in \mathbb{Z}$, we have $p_i \notin \{p_{i+1}, p_{i+2}\}$, and *closed* if M is the identity.

Let $\tilde{\mathcal{P}}_n$ denote the space of nondegenerate twisted discrete curves of length n . $\tilde{\mathcal{P}}_n$ is an open subvariety of $(\mathbb{P}^1)^n \times \mathrm{PGL}_2$, and PGL_2 acts on it by

$$A \cdot (p_1, p_2, \dots, p_n, M) = (A(p_1), A(p_2), \dots, A(p_n), AMA^{-1}).$$

The quotient $\mathcal{P}_n := \tilde{\mathcal{P}}_n / \mathrm{PGL}_2$ is the *moduli space of nondegenerate twisted curves of length n* . Given $p \in \tilde{\mathcal{P}}_n$, we define the c -variables

$$c_i := \mathrm{cr}(p_{i-1}, p_i, p_{i+2}, p_{i+1}) \text{ for all } i \in \mathbb{Z}. \quad (5)$$

Notice that $c_{i+n} = c_i$ for all $i \in \mathbb{Z}$. If p is nondegenerate, $c_i(p) \notin \{0, \infty\}$, so the c -variables give us a morphism

$$\begin{aligned} c : \tilde{\mathcal{P}}_n &\rightarrow (\mathbb{C}^\times)^n \\ p &\mapsto (c_1, c_2, \dots, c_n). \end{aligned} \quad (6)$$

Since each c_i is a cross-ratio, this morphism is PGL_2 invariant, and therefore (6) descends to a morphism $c : \mathcal{P}_n \rightarrow (\mathbb{C}^\times)^n$. Given the c -variables and three initial points p_1, p_2, p_3 , the whole discrete curve is recovered from (5). Since any three points can be mapped to any other three points by a projective transformation, the c -variables characterize a discrete curve up to projective transformations and so c is an isomorphism. The inverse morphism is given explicitly in [AFIT20, Section 3.2].

The following lemma gives an explicit representative for the PGL_2 conjugacy class of the monodromy matrix M in terms of the c -variables.

Theorem 2.1 ([AFIT20, Lemma 3.2]).

$$M = \begin{bmatrix} 0 & c_1 \\ -1 & 1 \end{bmatrix} \begin{bmatrix} 0 & c_2 \\ -1 & 1 \end{bmatrix} \cdots \begin{bmatrix} 0 & c_n \\ -1 & 1 \end{bmatrix}$$

represents the monodromy matrix.

2.3 The Poisson variety \mathcal{U}_n .

Let $\vec{\alpha} = (\alpha_i)_{i \in \mathbb{Z}}$ with $\alpha_i \in \mathbb{C} \setminus \{0, 1\}$ such that $\alpha_{i+n} = \alpha_i$. Two discrete curves $p, q \in \tilde{\mathcal{C}}_n$ are said to be $\vec{\alpha}$ -related, and denoted $p \vec{\alpha} \sim q$ if

$$\mathrm{cr}(p_i, q_i, p_{i+1}, q_{i+1}) = \alpha_i \text{ for all } i \in \mathbb{Z}, \quad (7)$$

and p and q have the same monodromy. Note that condition (7) alone does not imply that p and q have the same monodromy. The relation $\vec{\alpha} \sim$ is PGL_2 invariant and therefore descends to a relation

on \mathcal{P}_n . If $\alpha_i = \alpha$ for all i , then we say that p and q are α -related and write $p \overset{\vec{\alpha}}{\sim} q$.

Let $\tilde{\mathcal{U}}_n$ denote the space of pairs of $\vec{\alpha}$ -related nondegenerate twisted curves of length n . It is a subvariety of $(\mathbb{P}^1)^{2n} \times \mathrm{PGL}_2$ and PGL_2 acts on it by

$$A \cdot (p_1, \dots, p_n, q_1, \dots, q_n, M) = (A(p_1), \dots, A(p_n), A(q_1), \dots, A(q_n), AMA^{-1}).$$

We define the u -variables

$$u_i = -\mathrm{cr}(p_i, p_{i+1}, q_i, p_{i-1}) \text{ for all } i \in \mathbb{Z}. \quad (8)$$

Since p and q are nondegenerate and $\vec{\alpha}$ -related, $u_i \notin \{0, -1, \infty\}$. Therefore the u -variables define a PGL_2 invariant morphism $u : \tilde{\mathcal{U}}_n \rightarrow (\mathbb{C} \setminus \{0, -1\})^n$ which descends to a morphism

$$u : \mathcal{U}_n := \tilde{\mathcal{U}}_n / \mathrm{PGL}_2 \rightarrow (\mathbb{C} \setminus \{0, -1\})^n.$$

Consider the morphism

$$\begin{aligned} \rho_{\vec{\alpha}} : \mathcal{U}_n &\rightarrow \mathcal{P}_n \\ (p, q, M) &\mapsto (p, M). \end{aligned}$$

Remark. $\tilde{\mathcal{U}}_n$ and \mathcal{U}_n also depend on $\vec{\alpha}$, but we suppress this dependence in the notation.

In [AFIT20, Section 4.8] it is shown that

$$\begin{array}{ccc} \mathcal{U}_n & \xrightarrow{\rho_{\vec{\alpha}}} & \mathcal{P}_n \\ \downarrow u & & \downarrow c \\ (\mathbb{C} \setminus \{0, -1\})^n & \xrightarrow{\Lambda_{\vec{\alpha}}} & (\mathbb{C}^\times)^n \end{array}$$

commutes, where the map $\Lambda_{\vec{\alpha}}$ is determined by $c_i = \frac{\alpha_i}{(1+u_i)(1+\frac{1}{u_{i+1}})}$. If we are given u -variables, we can recover p up to projective transformations as $c^{-1} \circ \Lambda_{\vec{\alpha}}(u_1, \dots, u_n)$, and q is then determined by (8). Therefore the morphism u induces an isomorphism between \mathcal{U}_n and $(\mathbb{C} \setminus \{0, -1\})^n$. The set \mathcal{U}_n is the *moduli space of pairs of $\vec{\alpha}$ -related twisted discrete curves of length n* .

The Poisson bracket

$$\{u_i, u_{i+1}\}_{\mathcal{U}_n} := u_i u_{i+1},$$

makes $(\mathcal{U}_n, \{\cdot, \cdot\}_{\mathcal{U}_n})$ a Poisson variety while the Poisson bracket

$$\{c_i, c_{i+1}\}_{\vec{\alpha}} := c_i c_{i+1} \left(1 - \frac{c_i}{\alpha_i} - \frac{c_{i+1}}{\alpha_{i+1}}\right), \quad \{c_i, c_{i+2}\}_{\vec{\alpha}} := -\frac{1}{\alpha_{i+1}} c_i c_{i+1} c_{i+2}, \quad (9)$$

makes $(\mathcal{P}_n, \{\cdot, \cdot\}_{\vec{\alpha}})$ a Poisson variety. For both Poisson brackets, we only give the nonzero values obtained by pairing two coordinate functions. We also define the rescaled coordinates $\bar{c}_i := \frac{c_i}{\alpha_i}$. In these coordinates the Poisson bracket $\{\cdot, \cdot\}_{\vec{\alpha}}$ takes the simpler form

$$\{\bar{c}_i, \bar{c}_{i+1}\} = \bar{c}_i \bar{c}_{i+1} (1 - \bar{c}_i - \bar{c}_{i+1}), \quad \{\bar{c}_i, \bar{c}_{i+2}\} = -\bar{c}_i \bar{c}_{i+1} \bar{c}_{i+2}.$$

A computation similar to [AFIT20, Lemma 3.9] shows that $\rho_{\vec{\alpha}}$ is Poisson. [AFIT20, Corollary 2.7] shows that $\rho_{\vec{\alpha}}$ is generically finite of degree 2, that is for a generic discrete curve $p \in \mathcal{P}_n$ there are

two discrete curves $q, r \in \mathcal{P}_n$ that are $\vec{\alpha}$ -related to p . Therefore the map $T_{\vec{\alpha}} : (p, q, M) \mapsto (p, r, M)$ is a birational involution of \mathcal{U}_n . \mathcal{U}_n also has another involution $j : (p, q, M) \mapsto (q, p, M)$ given in coordinates by

$$u_i \mapsto v_i := \frac{1}{u_i} \frac{\alpha_i - 1}{\alpha_{i-1} - 1} = -\text{cr}(q_i, q_{i+1}, p_i, q_{i-1}). \quad (10)$$

2.4 Cross-ratio dynamics and integrability

Suppose $(q, M) \in \mathcal{P}_n$ such that $|\rho_{\vec{\alpha}}^{-1}(q, M)| = 2$, and suppose p, r are the two discrete curves $\vec{\alpha}$ -related to q . The birational automorphism

$$\begin{aligned} \nu_{\vec{\alpha}} &= T_{\vec{\alpha}} \circ j : \mathcal{U}_n \rightarrow \mathcal{U}_n \\ &(p, q, M) \mapsto (q, r, M) \end{aligned}$$

is called *cross-ratio dynamics*.

For $I \subset [n]$, let $c_I := \prod_{i \in I} c_i$. Similarly we define \bar{c}_I, α_I, u_I etc. Let $c_{\text{even}} := c_2 c_4 \dots$ and $c_{\text{odd}} := c_1 c_3 \dots$ denote the product of the even and odd c variables respectively. In the same way, we define α_{even} etc.

$I \subset [i, j]$ is said to be *cyclically sparse* if it contains no pair of consecutive indices where the indices are taken periodic modulo n . Define

$$F_k(c) = \sum_{I \text{ cyclically sparse: } |I|=k} c_I \text{ for } k = 0, \dots, \lfloor \frac{n}{2} \rfloor, \quad (11)$$

$$E_{\vec{\alpha}} = \frac{1}{\bar{c}_{[n]}} \left(\sum_{k=0}^{\lfloor \frac{n}{2} \rfloor} (-1)^k F_k(\bar{c}) \right)^2. \quad (12)$$

Theorem 2.2 ([AFIT20, Main Theorem 1]). *We have:*

1. For n even, $\{\cdot, \cdot\}_{\vec{\alpha}}$ has corank 2 and the subalgebra of Casimirs is generated by $E_{\vec{\alpha}}$ and $\frac{c_{\text{even}}}{c_{\text{odd}}}$.
2. For n odd, $\{\cdot, \cdot\}_{\vec{\alpha}}$ has corank 1 and the Casimir is $E_{\vec{\alpha}}$.
3. For $k = 1, 2, \dots, \lfloor \frac{n+1}{2} \rfloor - 1$, the functions $\frac{F_k(c)^2}{c_{[n]}}$ mutually commute and form a maximal set of functionally independent Hamiltonians, making the Poisson variety \mathcal{P}_n a Liouville integrable system.

Moreover, cross-ratio dynamics is discrete integrable in the following sense:

1. $\nu_{\vec{\alpha}}$ is Poisson.
2. The pullbacks of the Hamiltonians and the Casimirs to \mathcal{U}_n by $\rho_{\vec{\alpha}}$ are invariant under $\nu_{\vec{\alpha}}$.

The following theorem shows that the Hamiltonians can be obtained from the monodromy matrix.

Theorem 2.3 ([AFIT20, Theorem 1]). *We have*

$$\frac{1}{\det M} \text{tr}^2 M = \frac{1}{c_{[n]}} \left(\sum_{k=0}^{\lfloor \frac{n}{2} \rfloor} (-1)^k F_k(c) \right)^2.$$

Remark. Note that $\text{tr}M$ is not PGL_2 invariant, but the normalized trace $\frac{\text{tr}M}{\sqrt{\det M}}$ is. However the normalized trace is not a regular function on \mathcal{P}_n , so we need to square everything to make it so.

To get the Hamiltonians from Theorem 2.3, notice that $F_k(c)$ is the homogeneous degree k component of $\sqrt{c_{[n]}} \frac{\text{tr}M}{\sqrt{\det M}}$. This observation will be very useful in Section 6.2.

3 The dimer integrable system

For further details on this section, see [GK13].

3.1 The dimer model in a torus.

Let $\Gamma = (B \cup W, E)$ be a bipartite graph embedded in a torus \mathbb{T} such that $|B| = |W|$ and such that the faces of Γ , that is, the connected components of the complement of Γ , are disks. We denote by F the set of faces of Γ . An *edge weight* on Γ is a function $\text{wt} : E \rightarrow \mathbb{C}^\times$. Two edge weights wt_1 and wt_2 are said to be *gauge equivalent* if there is a function $g : B \cup W \rightarrow \mathbb{C}^\times$ such that for every edge $e = \{b, w\}$ with $b \in B, w \in W$, we have $\text{wt}_2(e) = \text{wt}_1(e)g(w)g(b)^{-1}$. Let \mathcal{L}_Γ denote the space of edge weights modulo gauge equivalence.

Equivalently, we can consider the graph Γ as a cell complex whose 0 and 1-cells are $B \cup W$ and E respectively. Considering each edge $e = bw$ to be oriented from b to w , we have the nonzero cellular chain groups

$$C_0(\Gamma, \mathbb{Z}) = \mathbb{Z}B \oplus \mathbb{Z}W, \quad C_1(\Gamma, \mathbb{Z}) = \mathbb{Z}E,$$

with boundary homomorphism $\partial : C_1(\Gamma, \mathbb{Z}) \rightarrow C_0(\Gamma, \mathbb{Z})$ given by $\partial(e) = w - b$, so that $H_1(\Gamma, \mathbb{Z}) = \text{Ker } \partial$. Dually, we have cellular cochain groups $C^q(\Gamma, \mathbb{C}^\times) := \text{Hom}_{\mathbb{Z}}(C_q(\Gamma, \mathbb{Z}), \mathbb{C}^\times)$, for $q \in \{0, 1\}$, with coboundary homomorphism $\delta : C^0(\Gamma, \mathbb{C}^\times) \rightarrow C^1(\Gamma, \mathbb{C}^\times)$ given by $\delta(g)(e) = \frac{g(w)}{g(b)}$. Since an edge weight is a 1-cochain and two edge weights are gauge equivalent if and only if they differ by a 1-coboundary, we have

$$\mathcal{L}_\Gamma = H^1(\Gamma, \mathbb{C}^\times) := C^1(\Gamma, \mathbb{C}^\times) / \delta(C^0(\Gamma, \mathbb{C}^\times)) \quad (13)$$

. We denote by $[\text{wt}]$ the cohomology class represented by the cochain wt .

For $[L] \in H_1(\Gamma, \mathbb{Z})$, we denote by $[\text{wt}]([L])$ the result of evaluating the cohomology class $[\text{wt}]$ on the homology class $[L]$ yielding an alternating product of edge weights around L . Explicitly, if the L is the 1-cycle $w_1 \xrightarrow{e_1} b_1 \xrightarrow{e_2} w_2 \xrightarrow{e_3} b_2 \xrightarrow{e_4} \dots \xrightarrow{e_{2n-2}} w_n \xrightarrow{e_{2n-1}} b_n \xrightarrow{e_{2n}} w_1 \in H_1(\Gamma, \mathbb{Z})$, we have

$$[\text{wt}]([L]) = \prod_{i=1}^n \frac{\text{wt}(e_{2i})}{\text{wt}(e_{2i-1})}.$$

Since $\mathcal{L}_\Gamma = \text{Hom}_{\mathbb{Z}}(H_1(\Gamma, \mathbb{Z}), \mathbb{C}^\times)$ is an algebraic torus, the algebra $\mathcal{O}_{\mathcal{L}_\Gamma}$ of regular functions on \mathcal{L}_Γ consists of the characters $\chi_{[L]}$ for $[L] \in H_1(\Gamma, \mathbb{Z})$ defined by $\chi_{[L]}([\text{wt}]) := [\text{wt}]([L])$.

We now give a description of $\mathcal{O}_{\mathcal{L}_\Gamma}$ in terms of a basis. For a face f of Γ , let ∂f denote the counterclockwise oriented cycle given by the walk along the boundary of f . Let a and b denote two cycles in Γ generating $H_1(\mathbb{T}, \mathbb{Z})$. Let $X_f := \chi_{[\partial f]}$. Then

$$\mathcal{O}_{\mathcal{L}_\Gamma} = \mathbb{C}[X_f^{\pm 1}, \chi_{[a]}^{\pm 1}, \chi_{[b]}^{\pm 1}] / (1 - \prod_{f \in F} X_f), \quad (14)$$

where the relation $\prod_{f \in F} X_f = 1$ comes from the relation $\sum_{f \in F} [\partial f] = 0$ in $H_1(\Gamma, \mathbb{Z})$.

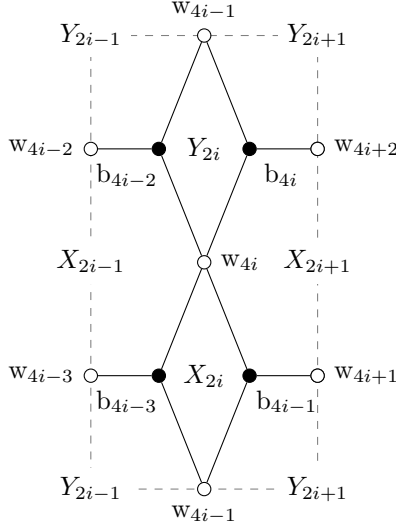


Figure 2: The building block graph G_i , which is a graph on a cylinder, since the top and bottom sides of the rectangle are identified. Each face is labeled by its face weight.

Example 3.1. For n even, consider the graph Γ_n in \mathbb{T} for which a fundamental domain is obtained by gluing the cylinder graphs G_i shown in Figure 2 for $i \in \{1, 2, \dots, \frac{n}{2}\}$ in the order $G_1 G_2 \cdots G_{\frac{n}{2}}$, so that w_{2n+1} is identified with w_1 and w_{2n+2} with w_2 . The faces of Γ_n are labeled by X_i, Y_i for $i \in \{1, 2, \dots, n\}$ as shown in Figure 2.

Zig-zag paths and Newton polygon. A *zig-zag* path in Γ is a path that turns maximally left at white vertices and maximally right at black vertices. Let \mathcal{Z} denote the set of zig-zag paths of Γ . Each zig-zag path $\beta \in \mathcal{Z}$ defines a homology class $[\beta] \in H_1(\mathbb{T}, \mathbb{Z})$. Label the zig-zag paths $\beta_1, \beta_2, \dots, \beta_{|\mathcal{Z}|}$ so that the $[\beta_i]$ regarded as vectors in $H_1(\mathbb{T}, \mathbb{Z}) \otimes \mathbb{R} \cong \mathbb{R}^2$ are in counterclockwise order. We construct a closed convex integral polygon $N(\Gamma)$ (or just N when Γ is clear from the context) by placing the $[\beta_i]$ such that the head of $[\beta_i]$ is the tail of $[\beta_{i+1}]$. Each edge of Γ is contained in two zig-zag paths that traverse the edge in opposite directions, so we have $\sum_{\beta \in \mathcal{Z}} [\beta] = 0$, which shows that N constructed as above is a closed polygon. N is unique up to translation and is called the Newton polygon of Γ . The name Newton polygon will be justified at the end of this section by that fact that this polygon arises as the Newton polygon of the characteristic polynomial. By construction, the set of primitive edge vectors of N is in bijection with \mathcal{Z} , but this bijection is not canonical when there is more than one zig-zag path with the same homology class.

A graph Γ is said to be *minimal* if any lift of a zig-zag path to the universal cover of \mathbb{T} has no self intersections and any lifts of two zig-zag paths to the universal cover of \mathbb{T} do not form parallel bigons (pairs of zig-zag paths oriented the same way intersecting twice).

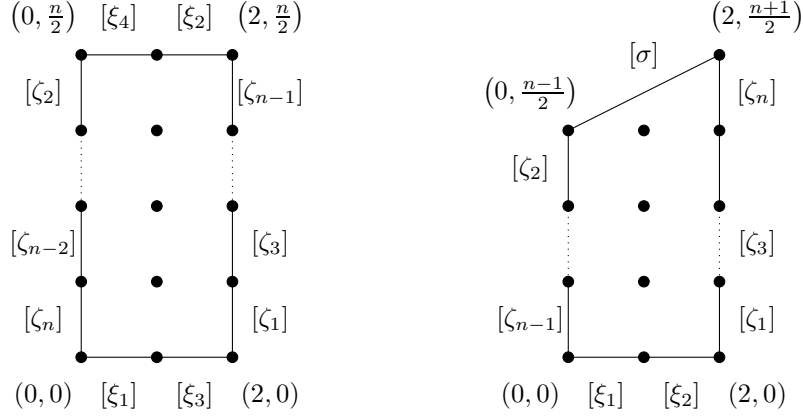


Figure 3: The Newton polygon of Γ_n for even n (left) and odd n (right).

Example 3.2. The graph Γ_n has $n + 4$ zig-zag paths:

$$\begin{aligned}
\xi_1 &= w_1, b_1, w_3, b_3, \dots, w_{2n-1}, b_{2n-1}, w_1, & [\xi_1] &= (1, 0), \\
\xi_2 &= w_1, b_{2n-1}, w_{2n}, b_{2n-3}, \dots, w_4, b_1, w_1, & [\xi_2] &= (-1, 0), \\
\xi_3 &= w_2, b_2, w_4, b_4, \dots, w_{2n}, b_{2n}, w_2, & [\xi_3] &= (1, 0), \\
\xi_4 &= w_2, b_{2n}, w_{2n-1}, b_{2n-2}, \dots, w_3, b_2, w_2, & [\xi_4] &= (-1, 0), \\
\zeta_{2i-1} &= w_{4i-1}, b_{4i-3}, w_{4i}, b_{4i-2}, w_{4i-1}, & [\zeta_{2i-1}] &= (0, 1), \\
\zeta_{2i} &= w_{4i-1}, b_{4i}, w_{4i}, b_{4i-1}, w_{4i-1}, & [\zeta_{2i}] &= (0, -1),
\end{aligned}$$

where $i \in \{1, 2, \dots, \frac{n}{2}\}$ and we use the basis (γ_z, γ_w) to identify $H_1(\mathbb{T}, \mathbb{Z})$ with \mathbb{Z}^2 (see Figure 5 for the case $n = 1$). Therefore the Newton polygon of Γ_n is (see Figure 3)

$$\text{Convex-hull} \left\{ (0, 0), (2, 0), \left(0, \frac{n}{2}\right), \left(2, \frac{n}{2}\right) \right\}.$$

It is easily checked that Γ_n is minimal.

Conjugate surface and Poisson structure. Thickening the edges of Γ , we obtain a ribbon graph. Equivalently a ribbon graph is a graph along with the data of a cyclic order of edges around each vertex. The ribbon graph obtained from Γ has the cyclic order induced from the embedding in \mathbb{T} . Let $\widehat{\Gamma}$ be the ribbon graph obtained from Γ by reversing the cyclic order at all white vertices. The boundary components of $\widehat{\Gamma}$ are in bijection with the zig-zag paths of Γ . Gluing in disks along these boundary components of $\widehat{\Gamma}$, we obtain a surface \widehat{S} called the *conjugate surface*, along with an embedding of Γ in \widehat{S} . Let $\epsilon_{\widehat{S}}$ denote the intersection form on $H_1(\widehat{S}, \mathbb{Z})$: For $[L_1], [L_2] \in H_1(\widehat{S}, \mathbb{Z})$, choose cycles L_1 and L_2 representing the homology classes and intersecting transversely. Then

$$\epsilon_{\widehat{S}}([L_1], [L_2]) = \sum_{p \in L_1 \cap L_2} \epsilon_p(L_1, L_2), \quad (15)$$

where $\epsilon_p(L_1, L_2)$ is the local intersection index, with sign chosen so that it is positive if L_2 crosses L_1 at p from its right side to its left side. The embedding $\iota : \Gamma \hookrightarrow \widehat{S}$ induces the homomorphism

of homology groups $\iota_* : H_1(\Gamma, \mathbb{Z}) \rightarrow H_1(\widehat{S}, \mathbb{Z})$. We define the alternating form ϵ_Γ on $H_1(\Gamma, \mathbb{Z})$ by $\epsilon_\Gamma([L_1], [L_2]) := \epsilon_{\widehat{S}}(\iota_*[L_1], \iota_*[L_2])$.

For $[L_1], [L_2] \in H_1(\Gamma, \mathbb{Z})$, define the Poisson bracket

$$\{\chi_{[L_1]}, \chi_{[L_2]}\}_\Gamma := \epsilon_\Gamma([L_1], [L_2])\chi_{[L_1]}\chi_{[L_2]}. \quad (16)$$

The faces of Γ in \widehat{S} become the zig-zag paths of Γ in \mathbb{T} , so we have $\{\chi_{[L_1]}, \chi_{[L_2]}\} = 0$ for all $[L_2]$ if and only if $[L_1] \in \bigoplus_{\beta \in \mathcal{Z}} \mathbb{Z} \cdot [\beta]$. Therefore the functions $C_\beta := \chi_{[\beta]}, \beta \in \mathcal{Z}$ generate the center of the Poisson algebra $\mathcal{O}_{\mathcal{L}_\Gamma}$. These functions are called *Casimirs*.

Elementary transformations and mutations. There are two local modifications of bipartite graphs called *elementary transformations* shown in Figure 7. An elementary transformation $s : \Gamma \rightarrow \Gamma'$ induces a unique up to isotopy homeomorphism of conjugate surfaces $\hat{s} : \widehat{S}_\Gamma \rightarrow \widehat{S}_{\Gamma'}$ [GK13, Lemma 4.1], which in turn induces an isomorphism $\hat{s}_* : H_1(\Gamma, \mathbb{Z}) \rightarrow H_1(\Gamma', \mathbb{Z})$. Associated to the elementary transformation s is a Poisson birational map of weights $\mu_s : \mathcal{L}_\Gamma \rightarrow \mathcal{L}_{\Gamma'}$:

1. The spider move s at face f : For $[L'] \in H_1(\Gamma', \mathbb{Z})$, let $[L] = (\hat{s}_*)^{-1}([L'])$. We define

$$\mu_s^*(\chi_{[L']}) = \chi_{[L]}(1 + X_f^{-\text{sign } \epsilon_\Gamma([L], \partial f)} - \epsilon_\Gamma([L], \partial f)). \quad (17)$$

2. Shrinking/expanding degree two vertices: We define $\mu_s^*(\chi_{[L']}) = \chi_{[L]}$.

Since elementary transformations are local, they do not change homology classes of zig-zag paths, and therefore the Newton polygon. Gluing the Poisson affine varieties \mathcal{L}_Γ for all Γ minimal with $N(\Gamma) = N$ using these Poisson birational maps, we obtain the Poisson space \mathcal{X}_N called the *dimer cluster Poisson variety* associated to N . \mathcal{X}_N is a cluster Poisson variety as defined by Fock and Goncharov [FG09], and will be the phase space of the dimer integrable system.

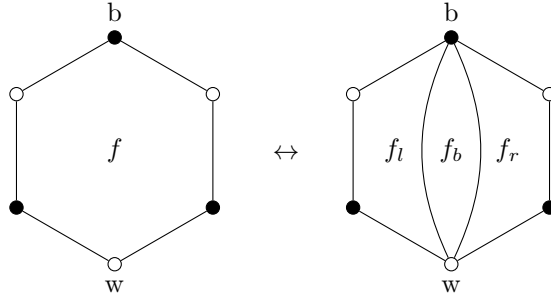


Figure 4: Adding/removing a bigon inside a face.

Inserting/removing a bigon. Figure 4 shows the insertion of a bigon between vertices $w \in W$ and $b \in B$ belonging to a common face f , with parameter t . This divides f into three new faces, the bigon f_b and the face f_l (resp. f_r) to the left (resp. right) of f_b when traversing the bigon from w to b . Let Γ_b denote the graph obtained. The embedding $i_b : \Gamma \hookrightarrow \Gamma_b$ induces a homomorphism $(i_b)_* : H_1(\Gamma, \mathbb{Z}) \rightarrow H_1(\Gamma_b, \mathbb{Z})$. We define the induced map of weights $\mu_t : \mathcal{L}_\Gamma \rightarrow \mathcal{L}_{\Gamma_b}$

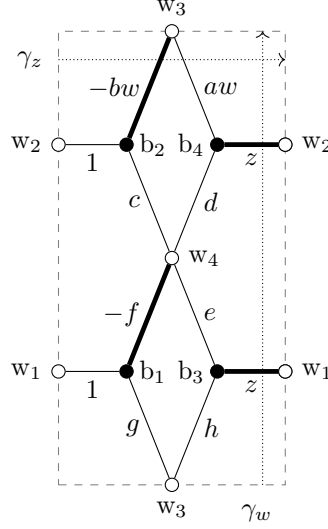


Figure 5: Edge weights, Kasteleyn sign and M_0 (thick edges) on Γ_2 .

on a basis as follows: If $[L]$ is topologically nontrivial in $H_1(\mathbb{T}, \mathbb{Z})$ or is the boundary of a face of Γ set $\mu_t^*(\chi_{(i_b)_*[L]}) = \chi_{[L]}$. Define also $\mu_t^*(X_{f_t}) = t$ and $\mu_t^*(X_{f_b}) = -1$. Note that the second equation implies that in any cocycle, the weights of the two edges of the bigon sum to zero. On the other hand, if we have bigon with $X_{f_b} = -1$, we may remove it. This induces a map of weights $\mu'_b : \{X_{f_b} = -1\} \rightarrow \mathcal{L}_\Gamma$, where $\{X_{f_b} = -1\}$ denotes the subvariety in \mathcal{L}_{Γ_b} , given by $\mu_b^*(\chi_{[L]}) = \chi_{(i_b)_*[L]}$.

3.2 Dimer covers and Kasteleyn theory.

A *dimer cover* M of Γ is a subset of E such that each vertex of Γ is incident to exactly one edge in M . Let \mathcal{M} denote the set of dimer covers of Γ . If we fix a reference dimer cover M_0 , then we can associate to each dimer cover a homology class

$$M \mapsto [M - M_0] \in H_1(\mathbb{T}, \mathbb{Z}),$$

where as before we orient $e = \{b, w\}$ from b to w . Given $[wt] \in \mathcal{L}_\Gamma$, each dimer cover also gets a *weight* $[wt](M - M_0)$. If Γ is minimal, we can describe the Newton polygon in terms of dimer covers.

Proposition 3.3 ([GK13, Theorem 3.12]). *For a minimal bipartite graph Γ in \mathbb{T} , we have*

$$N(\Gamma) = \text{Convex-hull} \{[M - M_0] : M \text{ is a dimer cover of } \Gamma\},$$

up to a translation.

Let R be a fundamental rectangle of \mathbb{T} and let γ_z, γ_w be cycles in \mathbb{T} such that $[\gamma_z], [\gamma_w]$ generate $H_1(\Gamma, \mathbb{Z})$. We choose γ_z, γ_w parallel to the sides of R as shown in Figure 5. Isotoping if necessary, we assume that the edges of Γ intersect γ_z, γ_w transversely. Applying $\text{Hom}_{\mathbb{Z}}(\cdot, \mathbb{C}^\times)$ to the surjection

$H_1(\Gamma, \mathbb{Z}) \rightarrow H_1(\mathbb{T}, \mathbb{Z})$, we get an inclusion $H^1(\mathbb{T}, \mathbb{C}^\times) \hookrightarrow H^1(\Gamma, \mathbb{C}^\times)$. Let $[\phi'] \in H^1(\Gamma, \mathbb{C}^\times)$ be in the image of $H^1(\mathbb{T}, \mathbb{C}^\times)$. In other words, $X_f([\phi']) = 1$ for all $f \in F$. We choose a cochain ϕ representing $[\phi']$ as follows: Let $z := [\phi']([\gamma_z])$, $w = [\phi']([\gamma_w])$, and define

$$\phi(e) := z^{(e, \gamma_w)} w^{(e, -\gamma_z)},$$

where (\cdot, \cdot) is the intersection index.

$[\kappa] \in H^1(\Gamma, \mathbb{C}^\times)$ is called a *Kasteleyn sign* if

1. $X_{[L]}([\kappa]) = \pm 1$ for all $[L] \in H_1(\Gamma, \mathbb{Z})$.
2. $X_f([\kappa]) = (-1)^{\frac{|\partial f|}{2}+1}$ for all $f \in F$, where $|\partial f|$ is the number of edges in ∂f .

Let $\kappa : E \rightarrow \mathbb{C}^\times$ be a cochain representing the Kasteleyn sign $[\kappa]$. We define the Kasteleyn matrix

$$K(z, w) : \mathbb{C}[z^{\pm 1}, w^{\pm 1}]^B \rightarrow \mathbb{C}[z^{\pm 1}, w^{\pm 1}]^W$$

by

$$K(z, w)_{\mathbf{w}, \mathbf{b}} := \sum_{e=\{\mathbf{b}, \mathbf{w}\} \in E} \text{wt}(e) \kappa(e) \phi(e).$$

Theorem 3.4 ([Kas63]). *We have*

$$\frac{1}{\text{wt}(M_0) \kappa(M_0) \phi(M_0)} \det K(z, w) = \sum_{M \in \mathcal{M}} \text{sign}([M - M_0]) [\text{wt}]([M - M_0]) [\phi]([M - M_0]),$$

where $\text{sign}([M - M_0])$ is a sign that depends on $[\kappa]$ and is irrelevant for our purposes.

Moreover,

$$P(z, w) := \frac{1}{\text{wt}(M_0) \kappa(M_0) \phi(M_0)} \det K(z, w)$$

is called the *characteristic polynomial* and $\Sigma := \{(z, w) \in (\mathbb{C}^\times)^2 : P(z, w) = 0\}$ is called the *spectral curve* of $(\Gamma, [\text{wt}])$. Although $K(z, w)$ depends on the choice of cochains representing $[\text{wt}]$ and $[\kappa]$, the spectral curve is independent of these choices. Moreover $N(\Gamma)$ is the Newton polygon of $P(z, w)$, that is, the convex hull of the pairs $(i, j) \in \mathbb{Z}^2$ such that $z^i w^j$ has a nonzero coefficient in $P(z, w)$.

Example 3.5. Consider the graph Γ_2 with edge-weights, Kasteleyn sign, ϕ and reference dimer cover M_0 as shown in Figure 5. The Kasteleyn matrix is

$$K(\Gamma_2) = \begin{bmatrix} \mathbf{b}_1 & \mathbf{b}_2 & \mathbf{b}_3 & \mathbf{b}_4 \\ 1 & 0 & z & 0 \\ 0 & 1 & 0 & z \\ g & -bw & h & aw \\ -f & c & e & d \end{bmatrix} \begin{matrix} \mathbf{w}_1 \\ \mathbf{w}_2 \\ \mathbf{w}_3 \\ \mathbf{w}_4 \end{matrix},$$

and the spectral curve is

$$P(z, w) = \frac{1}{bfz^2w} (-dh + (dg + ch)z - cgz^2 + aew + (be + af)zw + bfz^2w). \quad (18)$$

Hamiltonians. Let N° denote the interior of N . For $[\gamma] \in N^\circ \cap H_1(\Gamma, \mathbb{Z})$, let

$$H_{[\gamma]} := \sum_{M \in \mathcal{M}: [M - M_0] = [\gamma]} [\text{wt}]([M - M_0])$$

denote the coefficient of $[\phi]([\gamma])$ (up to a sign) in $P(z, w)$.

Proposition 3.6 ([GK13, Theorem 1.2]). *The generic level sets of the Casimirs are symplectic leaves of \mathcal{X}_N . The Hamiltonians $H_{[\gamma]}$ for $[\gamma] \in H_1(\mathbb{T}, \mathbb{Z}) \cap N^\circ$ mutually commute, making these symplectic leaves into algebraic integrable systems.*

4 The dimer model in a cylinder

Let $\Gamma_{\mathbb{A}} = (B \cup W, E)$ be a bipartite graph embedded in a cylinder \mathbb{A} such that:

1. The faces of $\Gamma_{\mathbb{A}}$ (including boundary faces) are disks.
2. Every vertex on the boundary of \mathbb{A} is white and of degree 1.
3. Let S and T denote the boundary white vertices on the two components of the boundary of \mathbb{A} , called the *source* and *target* vertices respectively. Let $W_{\text{int}} = W \setminus (S \cup T)$ denote the set of internal white vertices. We assume that $|S| = |T|$ and $|B| = |W| - |S|$.
4. $\Gamma_{\mathbb{A}}$ has a dimer cover M_0 that uses all the vertices in S and none of the vertices in T .

Here by a dimer cover of $\Gamma_{\mathbb{A}}$, we mean a matching that uses all the vertices in B and a $|B|$ -element subset of W exactly once. Note that assumptions 2 and 4 imply that the black vertices incident to the white vertices in S are all different. We call graphs $\Gamma_{\mathbb{A}}$ satisfying these conditions *balanced cylinder graphs*.

An *edge-weight* on $\Gamma_{\mathbb{A}}$ is a function $\text{wt} : E \rightarrow \mathbb{C}^\times$. Two edge weights wt_1 and wt_2 are *gauge equivalent* if there is a function $g : B \cup W \rightarrow \mathbb{C}^\times$ satisfying $g(w) = 1$ for all $w \in S \cup T$ such that for every edge $e = \{b, w\}$ with $b \in B, w \in W$, we have $\text{wt}_2(e) = g(b)^{-1} \text{wt}_1(e) g(w)$. In other words we only allow gauge transformations at interior vertices. The space of edge-weights modulo gauge transformations is the relative cohomology group $H^1(\Gamma_{\mathbb{A}}, S \cup T, \mathbb{C}^\times)$. As before, we denote by $[\text{wt}]$ the cohomology class represented by wt .

Let \mathcal{M} denote the set of dimer covers of $\Gamma_{\mathbb{A}}$. For $M \in \mathcal{M}$, we define its *weight* to be $\text{wt}(M) = \prod_{e \in M} \text{wt}(e)$. For $M \in \mathcal{M}$, let ∂M denote the set of boundary white vertices incident to M . For example, $\partial M_0 = S$.

4.1 Torus to cylinder

In this section, we outline a general procedure to construct a graph $\Gamma_{\mathbb{A}}$ in a cylinder satisfying the assumptions in Section 4 from a graph Γ in a torus \mathbb{T} . Let β be a zig-zag path in Γ . Without loss of generality, we assume that there are no 2-valent black vertices in β . Changing the fundamental domain if necessary, we can assume that $[\beta] = [\gamma_w]$. Split each black vertex in β to create a 2-valent white vertex. $[\gamma_w]$ has a representative cycle γ_w in \mathbb{T} that goes through each of the newly created 2-valent white vertices and does not intersect Γ anywhere else. Cutting \mathbb{T} along γ_w , we obtain a cylinder \mathbb{A} and a graph $\Gamma_{\mathbb{A}}$ embedded in it. The 2-valent white vertices become S and T , where T

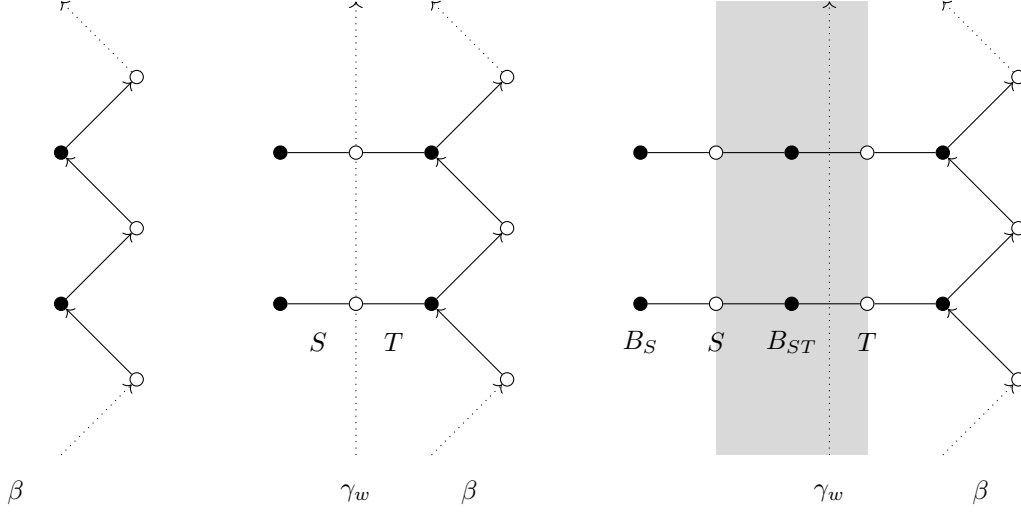


Figure 6: Cutting along a zig-zag path and labeling of vertices in Γ_{ST} . Removing the shaded region from \mathbb{T} , we get \mathbb{A} .

is connected to β (see Figure 6). Since $|B(\Gamma)| = |W(\Gamma)|$, we have $|B(\Gamma_{\mathbb{A}})| = |W(\Gamma_{\mathbb{A}})| - |S|$. There is a dimer cover M_0 in Γ that contains half the edges in β (see for example [GK13, Theorem 3.12]), which becomes a dimer cover in $\Gamma_{\mathbb{A}}$ such that $\partial M_0 = S$.

4.2 Kasteleyn theory in \mathbb{A}

Suppose $\Gamma_{\mathbb{A}}$ is a balanced cylinder graph. An element $[\kappa] \in H^1(\Gamma_{\mathbb{A}}, S \cup T, \mathbb{C}^\times)$ is called a *Kasteleyn sign* if

1. $X_{[L]}([\kappa]) = \pm 1$ for all $[L] \in H_1(\Gamma_{\mathbb{A}}, S \cup T, \mathbb{Z})$.
2. $X_f([\kappa]) = (-1)^{\frac{|\partial f|}{2}+1}$ for all $f \in F$, where $|\partial f|$ is the number of edges in ∂f .

The existence of a Kasteleyn sign is shown in [CR08]. Moreover there is the following version of Kasteleyn's theorem:

Theorem 4.1 ([CR08, Theorem 2.4]). *Let $I \subset S \cup T$ such that $|I| = |S|$, and let $K_{\mathbb{A}, I}$ denote the submatrix of the Kasteleyn matrix with rows indexed by white vertices in $I \cup W_{int}$ and columns indexed by black vertices in B . Then we have*

$$\frac{1}{\text{wt}(M_0)\kappa(M_0)} \det K_{\mathbb{A}, I} = \sum_{\partial M = I} \text{sign}([M - M_0])[\text{wt}([M - M_0])],$$

where $[M - M_0]$ is the relative homology class in $H_1(\mathbb{A}, \partial \mathbb{A}, \mathbb{Z})$ defined by the relative cycle $M - M_0$.

Let B_S denote the set of black vertices incident to S . B_S is matched to S by M_0 . The Kasteleyn

matrix $K_{\mathbb{A}}$ of $\Gamma_{\mathbb{A}}$ has the block matrix form

$$K_{\mathbb{A}} = \begin{bmatrix} B_S & B \setminus B_S \\ I & 0 \\ K_1 & K_2 \\ K_3 & K_4 \end{bmatrix} \begin{matrix} S \\ T \\ W_{\text{int}} \end{matrix}. \quad (19)$$

For generic $[\text{wt}]$, K_4 is invertible using Theorem 4.1 with $I = S$, since M_0 is a dimer cover with $\partial M_0 = S$ that will appear as a summand in $\det K_4 = \det K_{\mathbb{A},S}$. Define the Schur complement

$$\begin{aligned} L &:= K_{\mathbb{A}}/K_4 \\ &= \begin{bmatrix} I \\ K_1 \end{bmatrix} - \begin{bmatrix} 0 \\ K_2 \end{bmatrix} K_4^{-1} K_3 \\ &= \begin{bmatrix} I \\ \Pi \end{bmatrix}, \end{aligned} \quad (20)$$

where $\Pi := K_1 - K_2 K_4^{-1} K_3$. To get an explicit formula for the entries of Π , notice that for $w_i \in S, w_j \in T$, the square submatrix $L_{S \setminus \{w_i\} \cup \{w_j\}}$ of L with rows indexed by $S \setminus \{w_i\} \cup \{w_j\}$ is the Schur complement $K_{\mathbb{A}, S \setminus \{w_i\} \cup \{w_j\}}/K_4$. Using $\det K_4 = \det K_{\mathbb{A},S}$ and Theorem A.1, we have

$$\Pi_{w_j, b_i} = (-1)^{|S|-i} \det L_{S \setminus \{w_i\} \cup \{w_j\}} = (-1)^{|S|-i} \frac{\det K_{\mathbb{A}, S \setminus \{w_i\} \cup \{w_j\}}}{\det K_{\mathbb{A},S}}.$$

The Π matrix has the following multiplicativity property that is useful for explicit computations.

Proposition 4.2. *Suppose Γ is a graph obtained by gluing graphs Γ_i for $i = 1, \dots, n$ from left to right, so that $S(\Gamma_i)$ is identified with $T(\Gamma_{i+1})$. Then*

$$\Pi(\Gamma) = \Pi(\Gamma_1)\Pi(\Gamma_2) \cdots \Pi(\Gamma_n).$$

Here $S(\Gamma_i)$ and $T(\Gamma_{i+1})$ denote the source vertices of Γ_i and target vertices of Γ_{i+1} respectively.

We omit the proof since it is very similar to that of Theorem 4.4.

Remark. The matrix Π is closely related to the boundary measurement matrix of [GSTV16]. The reference dimer M_0 makes $\Gamma_{\mathbb{A}}$ into a directed network \mathcal{N} as follows: Orient each edge $e = bw$ contained in M_0 from $w \rightarrow b$, and assign it weight $\frac{1}{\text{wt}(e)}$, and each edge not contained in M_0 from $w \rightarrow b$ and assign it weight $\text{wt}(e)$. Each directed path in \mathcal{N} gets a weight that is the product of weights of all edges appearing in it. Then using Theorem 4.1, we have

$$\begin{aligned} \frac{1}{\text{wt}(M_0)\kappa(M_0)} \det K_{\mathbb{A},S} \Pi_{w_j, b_i} &= (-1)^{|S|-i} \frac{\det K_{\mathbb{A}, S \setminus \{w_i\} \cup \{w_j\}}}{\text{wt}(M_0)\kappa(M_0)} \\ &= (-1)^{|S|-i} \sum_{\partial M = S \setminus \{w_i\} \cup \{w_j\}} \text{sign}([M - M_0])[wt]([M - M_0]). \end{aligned}$$

Notice that if $\partial M = S \setminus \{w_i\} \cup \{w_j\}$, then $M - M_0$ is a directed path in \mathcal{N} from w_i to w_j , so $\frac{1}{\text{wt}(M_0)\kappa(M_0)} \det K_{\mathbb{A},S} \Pi$ is the boundary measurement matrix of \mathcal{N} . This is the reason for calling S and T the source and target vertices respectively.

Example 4.3. Consider the graph Γ_2 from Figure 5. Let $\Gamma_{\mathbb{A},2}$ denote the graph in the cylinder obtained from Γ_2 by applying the construction in Section 4.1 with the zig-zag path ζ_2 . In this case, we simply cut along the vertical side of the fundamental rectangle. The sources are the two white vertices w_1 and w_2 on the right boundary, while the targets are their copies on the left boundary that we denote by w_5 and w_6 . The set B_S is $\{b_3, b_4\}$. The Kasteleyn matrix is

$$K_{\mathbb{A}} = \begin{array}{cccc} & b_3 & b_4 & b_1 & b_2 \\ \left[\begin{array}{cccc} 1 & 0 & 0 & 0 \\ 0 & 1 & 0 & 0 \\ 0 & 0 & 1 & 0 \\ 0 & 0 & 0 & 1 \\ h & a & g & -b \\ e & d & -f & c \end{array} \right] & \begin{array}{l} w_1 \\ w_2 \\ w_5 \\ w_6 \\ w_3 \\ w_4 \end{array} \end{array},$$

and

$$\Pi = \frac{1}{bf - cg} \begin{bmatrix} ch + be & ac + bd \\ eg + fh & dg + af \end{bmatrix}. \quad (21)$$

4.3 Spectral curve of Γ from $\Gamma_{\mathbb{A}}$.

We now show how the spectral curve of Γ can be constructed from $\Gamma_{\mathbb{A}}$. In Γ , split the white vertices that are in the image of S and T under the projection of $\Gamma_{\mathbb{A}}$ to \mathbb{T} , so that we now have two copies of these white vertices which we identify with S and T respectively, connected by degree two black vertices. Let Γ_{ST} denote the graph obtained. Let B_{ST} denote the newly created degree two black vertices. Perturb γ_w so that it goes transversely through all the edges connecting B_{ST} with T (see Figure 6). Let $K_{\mathbb{A}}(w)$ denote the Kasteleyn matrix for $\Gamma_{\mathbb{A}}$ with weight $\text{wt}(e)w^{(e, -\gamma_z)}$, and let $\Pi(w)$ denote the matrix in (20). We extend a Kasteleyn sign κ on Γ to Γ_{ST} by defining $\kappa(e) = 1$ if e is an edge between B_{ST} and T and $\kappa(e) = -1$ if e is an edge between B_{ST} and S .

Theorem 4.4. $\Sigma = \{(z, w) \in (\mathbb{C}^\times)^2 : \det(zI + \Pi(w)) = 0\}$ is the spectral curve.

Proof. The Kasteleyn matrix $K(z, w)$ of Γ_{ST} has the block matrix form

$$K(z, w) = \begin{array}{c} B(\Gamma_{\mathbb{A}}) \\ K_{\mathbb{A}}(w) \end{array} \left[\begin{array}{c} B_{ST} \\ -I \\ zI \\ 0 \end{array} \right] \begin{array}{c} S \\ T \\ W_{\text{int}} \end{array}.$$

So we have (with B_S, K_4 as in (19))

$$K(z, w)/K_4 = \begin{array}{c} B_S \\ \Pi(w) \end{array} \left[\begin{array}{c} B_{ST} \\ -I \\ zI \end{array} \right] \begin{array}{c} S \\ T \end{array}.$$

By Theorem A.1, we get $\det K(z, w) = \det K_4 \det(zI + \Pi(w))$. □

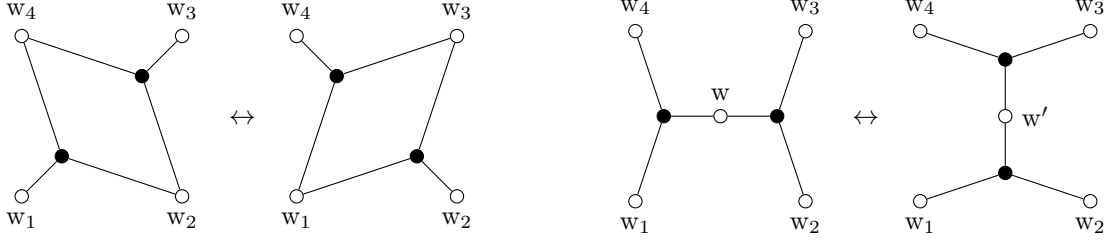


Figure 7: Elementary transformations allowed in TCD maps: spider move (left) and resplit (right).

Example 4.5. Consider again Γ_2 for which we have

$$\Pi(w) = \frac{1}{-cg + bfw} \begin{bmatrix} ch + bew & (ac + bd)w \\ eg + fh & dg + afw \end{bmatrix}$$

from (21). We have

$$\det(zI + \Pi(w)) = \frac{1}{-cg + bfw} (aew + afwz + bewz + bfwz^2 - cgz^2 + chz + dgz - dh),$$

which agrees with (18).

5 TCD maps on cylinders

5.1 TCD maps

We now describe the cokernel of K from a projective point of view in terms of *triple crossing diagram maps*, which we abbreviate to TCD maps. Let Γ be an arbitrary bipartite graph (not necessarily embedded on a torus) with $|W| > |B|$. Assume that the black vertices of Γ are all trivalent, which we can always do using split and join moves. A TCD map is a collection of points $(P_w)_{w \in W} \in \mathbb{CP}^{|W|-|B|-1}$ such that for each $b \in B$, the three points P_w for w incident to b are distinct and are all contained in a line.

Given a generic weight wt on Γ , we obtain a TCD map as follows: consider the exact sequence

$$0 \rightarrow \mathbb{C}^B \xrightarrow{K} \mathbb{C}^W \rightarrow \text{coker } K \rightarrow 0,$$

where $\text{coker } K$ is $(|W| - |B|)$ -dimensional. Let $v_w \in \text{coker } K$ be the image of e_w . Then the projectivizations P_w of the vectors v_w define a TCD map. Clearly the definition is invariant under gauge equivalence. On the other hand, given a TCD map, we recover the edge-weights modulo gauge transformations from the equations of the lines associated to the black vertices.

Remark. Note that the cokernel is only defined up to isomorphism. Different choices for a representative of the isomorphism class of the cokernel give different TCD maps related by projective transformations.

The advantage of working with Γ with trivalent black vertices is that we can keep track of both the geometric dynamics and the invariants while performing local moves. For TCD maps there are only two allowed elementary transformations, the spider move and the resplit, see Figure 7. In a generic situation, the points associated to white vertices after one of these two moves are determined by the combinatorics. Indeed, no points change when performing the spider move and the new point appearing in the resplit is determined as the intersection of the two lines represented by the two black vertices. It is a straight-forward calculation to verify that the edge-weights of Γ are compatible with the geometric constraints. In \mathbb{CP}^1 however, there is no incidence geometry. In this case, we *define* the new white vertex in the resplit such that the edge-weights correspond to a local move as dictated by the dimer model. Another useful property of TCD maps is that the face-variables can be recovered as multi-ratios as stated in the following Lemma.

Lemma 5.1 ([AGPR19, Proposition 2.6]). *For a loop $L = w_1 \rightarrow b_1 \rightarrow w_2 \rightarrow b_2 \rightarrow \dots \rightarrow w_n \rightarrow b_n \rightarrow w_1$, let w'_i denote the third white vertex incident to b_i that is not in $\{w_i, w_{i+1}\}$. Then we have*

$$[\text{wt}]([L]) = [\kappa]([L])^{-1} \text{mr}(P_{w_1}, P_{w'_1}, P_{w_2}, P_{w'_2}, \dots, P_{w_n}, P_{w'_n}).$$

Moreover, we make the following observation. Assume the white vertices are labeled as in Figure 7. Then

$$\text{mr}(P_{w_1}, P_w, P_{w_2}, P_{w_3}, P_{w'}, P_{w_4}) = -1 \quad (22)$$

holds. Note that this equation has a high degree of symmetry, it also holds if we swap $w \leftrightarrow w'$ or $w_1 \leftrightarrow w_3$ or $w_2 \leftrightarrow w_4$.

5.2 TCD map on $\Gamma_{\widehat{\mathbb{A}}}$ from Γ

Suppose $\Gamma_{\mathbb{A}}$ is a graph in \mathbb{A} obtained from a graph Γ in \mathbb{T} as in Section 4.1. We assume further that there is a dimer cover M_1 such that $\partial M_1 = T$, or equivalently that the matrix Π in (20) is invertible.

Let $\widehat{\mathbb{A}} := H_1(\mathbb{T}, \mathbb{R})/\mathbb{Z}[\gamma_w]$ denote the infinite cylinder covering \mathbb{A} . Note that $\widehat{\mathbb{A}} = \bigcup_{k \in \mathbb{Z}} \mathbb{A} + k[\gamma_z]$, that is $\widehat{\mathbb{A}}$ is obtained by gluing together infinitely many copies of \mathbb{A} . Let

$$\Gamma_{\widehat{\mathbb{A}}} = (B(\Gamma_{\widehat{\mathbb{A}}}) \cup W(\Gamma_{\widehat{\mathbb{A}}}), E(\Gamma_{\widehat{\mathbb{A}}})) \quad (23)$$

denote the preimage of Γ under the covering map $\widehat{\mathbb{A}} \rightarrow \mathbb{T}$. Fix a white vertex $w \in W(\Gamma_{\widehat{\mathbb{A}}})$ and choose a large enough m so that w is in $\mathbb{A}_m := \bigcup_{k \in [-m, m] \cap \mathbb{Z}} (\mathbb{A} + k\gamma_z) \subset \widehat{\mathbb{A}}$. Let $\Gamma_{\mathbb{A}_m} := \Gamma_{\widehat{\mathbb{A}}} \cap \mathbb{A}_m$.

Lemma 5.2. *We have $\text{coker } K_{\mathbb{A}_m} \cong \text{coker } K_{\mathbb{A}} \cong \mathbb{C}^{|W|-|B|}$ for all $m \geq 0$. Moreover with these identifications, the image of e_w in $\mathbb{C}^{|W|-|B|}$ under the cokernel map of $K_{\mathbb{A}_m}$ is independent of m , where e_w is the unit basis vector corresponding to w in $\mathbb{C}^{W(\Gamma_{\mathbb{A}_m})}$.*

Proof. Suppose $m > m'$. $K_{\mathbb{A}_m}$ has the block form

$$K_{\mathbb{A}_m} = \begin{bmatrix} B(\Gamma_{\mathbb{A}_{m'}}) & B(\Gamma_{\mathbb{A}_m}) \setminus B(\Gamma_{\mathbb{A}_{m'}}) \\ K_{\mathbb{A}_{m'}} & * \\ 0 & K' \end{bmatrix} \begin{matrix} W(\Gamma_{\mathbb{A}_{m'}}) \\ W(\Gamma_{\mathbb{A}_m}) \setminus W(\Gamma_{\mathbb{A}_{m'}}) \end{matrix},$$

where K' is invertible by existence of M_0 and M_1 , and Theorem 4.1. Therefore $K_{\mathbb{A}_m}/K' = K_{\mathbb{A}_{m'}}$, and so the second statement follows from Theorem A.2. By Theorem A.2 with $m' = 0$ we get $\text{coker } K_{\mathbb{A}_m} \cong \text{coker } K_{\mathbb{A}} \cong \mathbb{C}^{|W|-|B|}$ for all $m \geq 0$. \square

We define a TCD map $P : W(\Gamma_{\widehat{\mathbb{A}}}) \rightarrow \mathbb{C}P^{|W(\Gamma_{\mathbb{A}})|-|B(\Gamma_{\mathbb{A}})|-1}$ as follows: For $w \in W(\Gamma_{\widehat{\mathbb{A}}})$, we choose m sufficiently large so that $w \in W(\Gamma_{\mathbb{A}_m})$. Let v_w denote the image of e_w in $\mathbb{C}^{|W(\Gamma_{\mathbb{A}})|-|B(\Gamma_{\mathbb{A}})|}$ as in Lemma 5.2, and define $P_w \in \mathbb{C}P^{|W(\Gamma_{\mathbb{A}})|-|B(\Gamma_{\mathbb{A}})|-1}$ to be the projectivization of v_w . Lemma 5.2 guarantees that the definition is independent of the choice of m .

5.3 Monodromy of a TCD map on $\Gamma_{\widehat{\mathbb{A}}}$

A pair (P, M) where $P : W(\Gamma_{\widehat{\mathbb{A}}}) \rightarrow \mathbb{C}P^{|W(\Gamma_{\mathbb{A}})|-|B(\Gamma_{\mathbb{A}})|-1}$ is a TCD map and $M \in \text{PGL}_{|W(\Gamma_{\mathbb{A}})|-|B(\Gamma_{\mathbb{A}})|}$ is called a *twisted TCD map* if $M(P_w) = P_{w+\gamma_z}$ for all $w \in W(\Gamma_{\widehat{\mathbb{A}}})$. M is called the *monodromy* of P .

Now suppose $P : W(\Gamma_{\widehat{\mathbb{A}}}) \rightarrow \mathbb{C}P^{|W(\Gamma_{\mathbb{A}})|-|B(\Gamma_{\mathbb{A}})|-1}$ is a TCD map on $\Gamma_{\widehat{\mathbb{A}}}$ as in Section 5.2. The existence of M_1 means that the map $\mathbb{C}^T \rightarrow \text{coker } K_{\mathbb{A}}$ given by $e_w \mapsto v_w$ is an isomorphism. In other words, this map defines a change of basis for $\text{coker } K_{\mathbb{A}}$ making $v_w, w \in T$ the standard basis vectors. Let $[\Pi]$ denote the class of Π in $\text{PGL}_{|W(\Gamma_{\mathbb{A}})|-|B(\Gamma_{\mathbb{A}})|}$, where Π is the matrix in (20).

Proposition 5.3. *P is a twisted TCD map. The $\text{PGL}_{|W(\Gamma_{\mathbb{A}})|-|B(\Gamma_{\mathbb{A}})|}$ -matrix $[\Pi]$ is the monodromy of P in the basis $\{v_w\}_{w \in T}$.*

Proof. Let $T = \{w_1, \dots, w_n\}$ be the set of target vertices in $W(\Gamma_{\mathbb{A}})$. Since $\begin{bmatrix} I \\ \Pi \end{bmatrix}$ is the Schur complement of $K_{\mathbb{A}}$, by Theorem A.2 we have

$$\begin{bmatrix} v_{w_1+\gamma_z} & \cdots & v_{w_n+\gamma_z} & v_{w_1} & \cdots & v_{w_n} \end{bmatrix} \begin{bmatrix} I \\ \Pi \end{bmatrix} = 0,$$

where v_{w_i} is the standard basis vector e_i . From this, we get $v_{w_i+\gamma_z} = -\Pi v_{w_i}$. The same argument applied to the translated graph $\Gamma_{\mathbb{A}+k\gamma_z}$ gives $v_{w_i+(k+1)\gamma_z} = -\Pi v_{w_i+k\gamma_z}$. This implies $v_{w_i+k\gamma_z} = (-\Pi)^k v_{w_i}$ for all $k \in \mathbb{Z}$. For $w \in W(\Gamma_{\mathbb{A}})$, since $\{v_{w_i}\}$ is a basis, there exists a_i such that $v_w = \sum_{i=1}^n a_i v_{w_i}$. Then we have

$$\begin{aligned} (-\Pi)^k v_w &= \sum_{i=1}^n a_i (-\Pi)^k v_{w_i} \\ &= \sum_{i=1}^n a_i v_{w_i+k\gamma_z} \\ &= v_{w+k\gamma_z}, \end{aligned}$$

where the last equality follows from $K_{\mathbb{A}} = K_{\mathbb{A}+k\gamma_z}$. Any white $w' \in W(\Gamma_{\widehat{\mathbb{A}}})$ is of the form $w + m\gamma_z$ for some $w \in W(\Gamma_{\mathbb{A}})$. Then $w' + \gamma_z = w + (m+1)\gamma_z$, so that we have

$$v_{w'} = (-\Pi)^m v_w, \quad v_{w'+\gamma_z} = (-\Pi)^{m+1} v_w,$$

and therefore $v_{w'+\gamma_z} = -\Pi v_{w'}$. Projectivizing, we get the statement of the proposition. \square

6 Twisted TCD maps from \mathcal{U}_n for n even

For n even, recall the graph Γ_n from Example 3.1 and let N denote its Newton polygon computed in Example 3.2. Suppose the faces and zig-zag paths of Γ_n are labeled as in Figure 2 and Example 3.2 respectively. The set $\{X_1, \dots, X_n, Y_1, \dots, Y_n, \chi_{[\zeta_1]}, \chi_{[\xi_1]}\}$ is a set of generators for $\mathcal{O}_{\mathcal{L}_{\Gamma_n}}$ and the only relation among them is $\prod_{i=1}^n X_i Y_i = 1$.

Let $\mathcal{X}_{N, \bar{\alpha}}$ (resp. $\mathcal{L}_{\Gamma_n, \bar{\alpha}}$) denote the subvariety of \mathcal{X}_N (resp. \mathcal{L}_{Γ_n}) where

$$\chi_{[\zeta_{2i-1}]} = 1 - \alpha_{2i-1}, \quad (24)$$

$$\chi_{[\zeta_{2i}]} = \frac{1}{1 - \alpha_{2i}}, \quad (25)$$

for all $i \in \{1, 2, \dots, n\}$. Recall from Section 2 that $\mathcal{U}_n \cong (\mathbb{C} \setminus \{0, -1\})^n$.

Definition 6.1. We define a rational map

$$\pi_{\bar{\alpha}} : \mathcal{X}_{N, \bar{\alpha}} \supset \mathcal{L}_{\Gamma_n, \bar{\alpha}} \rightarrow (\mathbb{C} \setminus \{0, -1\})^n \quad (26)$$

such that

$$\pi_{\bar{\alpha}}^* u_i = Y_i, \quad (27)$$

for all $i \in \{1, 2, \dots, n\}$.

Lemma 6.2. *We have*

$$\pi_{\bar{\alpha}}^* v_i = X_i$$

for all $i \in \{1, 2, \dots, n\}$.

Proof. It follows from

$$X_i Y_i = \begin{cases} \chi_{[\zeta_i]} \chi_{[\zeta_{i-1}]} & \text{if } i \text{ is odd;} \\ \frac{1}{\chi_{[\zeta_i]} \chi_{[\zeta_{i-1}]}} & \text{if } i \text{ is even,} \end{cases}$$

and the equations (24), (25) and (10). \square

Next, we check that:

Lemma 6.3. $\pi_{\bar{\alpha}}$ is Poisson.

Proof. Y_1, Y_2, \dots, Y_n and $\chi_{[\xi_1]}$ are coordinates on $\mathcal{X}_{N, \bar{\alpha}}$. The only nonzero Poisson brackets on $\mathcal{X}_{N, \bar{\alpha}}$ in these coordinates are

$$\{Y_i, Y_{i+1}\} = Y_i Y_{i+1}, \quad i = 1, 2, \dots, n. \quad (28)$$

We compute that

$$\pi_{\bar{\alpha}}^* \{Y_i, Y_{i+1}\} = \pi_{\bar{\alpha}}^* (Y_i Y_{i+1}) = u_i u_{i+1} = \{\pi_{\bar{\alpha}}^* Y_i, \pi_{\bar{\alpha}}^* Y_{i+1}\}. \quad (29)$$

\square

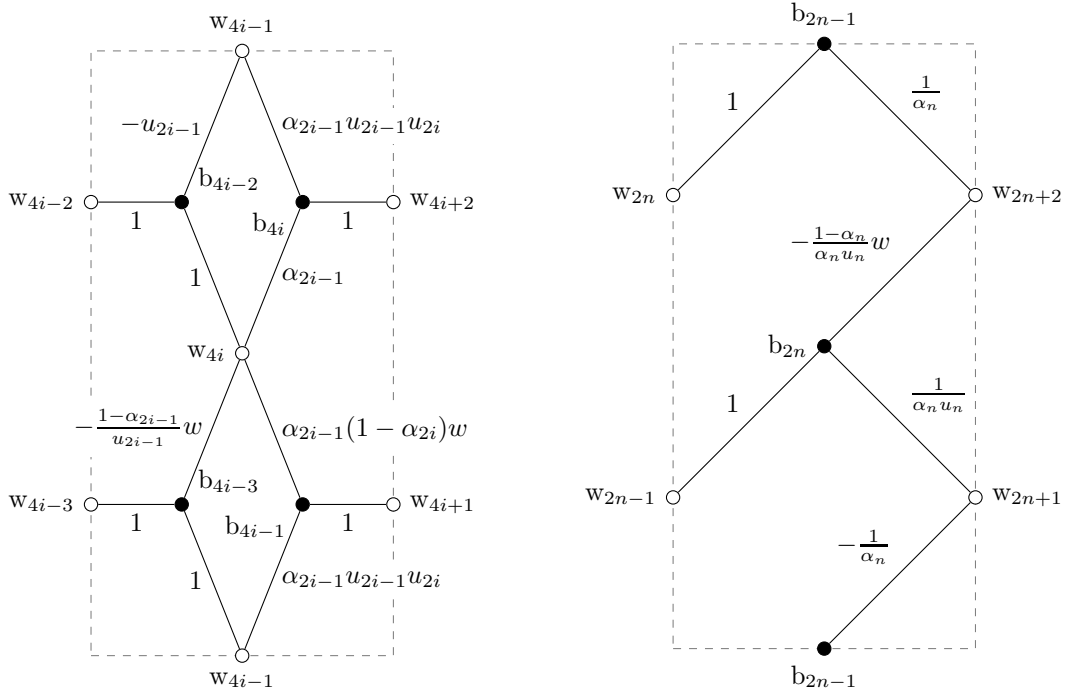


Figure 8: Edge weights and Kasteleyn signs for the building block graphs G_i (left) as well as G_n^{odd} (right).

6.1 TCD map and the pair of curves

Let $[\text{wt}] \in \mathcal{X}_{N, \bar{\alpha}}$ such that $u^{-1} \circ \pi_{\bar{\alpha}}([\text{wt}]) = (p, q, M)$. We choose edge weights representing $[\text{wt}]$ and Kasteleyn signs as in Figure 8.

Remark. We have additionally the freedom to choose $\chi_{\xi_1}([\text{wt}])$. However this is a Casimir and for our purposes may be absorbed into z since it changes the Hamiltonians by a multiplicative factor, and does not affect the TCD map.

Note that we have $|W(\Gamma_{n, \mathbb{A}})| - |B(\Gamma_{n, \mathbb{A}})| = 2$. Let $P : \Gamma_{n, \hat{\mathbb{A}}} \rightarrow \mathbb{CP}^1$ denote the TCD map associated to $[\text{wt}]$. $\Gamma_{n, \hat{\mathbb{A}}}$ is a union of infinitely many copies of the building block graph $G_i, i \in \mathbb{Z}$. We label the vertices of $\Gamma_{n, \hat{\mathbb{A}}}$ as in Figure 2.

Lemma 6.4. *We have (see Figure 1)*

$$P_{w_k} = \begin{cases} q_{2i-1} & \text{if } k = 4i - 3; \\ q_{2i} & \text{if } k = 4i - 1; \\ p_{2i-1} & \text{if } k = 4i - 2; \\ p_{2i} & \text{if } k = 4i, \end{cases}$$

up to a projective transformation, for all $i \in \mathbb{Z}$.

Proof. The discrete curves p and q are determined up to projective transformations by the cross-ratios (7) and (8). Using Lemma 5.1, we see from (31) and Lemma 6.2 that the P_w have the same cross-ratios. \square

Corollary 6.5. *The monodromy matrix of the TCD map P coincides with the monodromy matrix M of the pair of discrete curves p, q .*

We now compute the monodromy matrix. The Kasteleyn matrix of G_i is

$$K_{G_i}(w) = \begin{bmatrix} 1 & 0 & 0 & 0 \\ 0 & 1 & 0 & 0 \\ 0 & 0 & 1 & 0 \\ 0 & 0 & 0 & 1 \\ \alpha_{2i-1}u_{2i-1}u_{2i} & \alpha_{2i-1}u_{2i-1}u_{2i} & 1 & -u_{2i-1} \\ \alpha_{2i-1}1 - \alpha_{2i}w & \alpha_{2i-1} & -\frac{1-\alpha_{2i-1}}{u_{2i-1}}w & 1 \end{bmatrix}$$

so that

$$\Pi_{G_i}(w) = \frac{\alpha_{2i-1}}{(1 - \alpha_{2i-1})w - 1} \begin{bmatrix} u_{2i-1}(u_{2i} + (1 - \alpha_{2i})w) & u_{2i-1}(1 + u_{2i}) \\ (1 - \alpha_{2i})w + u_{2i}(1 - \alpha_{2i-1})w & 1 + u_{2i}(1 - \alpha_{2i-1})w \end{bmatrix}.$$

We have $\det \Pi_{G_i}(w) = \left(\frac{\alpha_{2i-1}}{(1 - \alpha_{2i-1})w - 1} \right) ((1 - \alpha_{2i})w - 1) \alpha_{2i-1} u_{2i-1} u_{2i}$. By Proposition 4.2, the monodromy matrix is

$$\Pi(w) = \Pi_{G_1}(w) \Pi_{G_2}(w) \cdots \Pi_{G_{\frac{n}{2}}}(w)$$

and so we get

$$\det \Pi(1) = \alpha_{[n]} u_{[n]}. \quad (30)$$

6.2 Hamiltonians

The following lemma is elementary.

Lemma 6.6. *Suppose M is a 2×2 matrix and $P(z) = \det(zI + M)$ is its characteristic polynomial. Then $P(z) = z^2 + \text{tr } Mz + \det M$.*

Let $P(z, w)$ denote the characteristic polynomial of Γ_n , normalized so that it has Newton polygon as in Figure 3 with the vertex in top right corner corresponding to $z^2 w^{\frac{n}{2}}$, and such that the coefficient of $z^2 w^{\frac{n}{2}}$ is $\frac{1}{\alpha_{\text{odd}}} \prod_{i=1}^{\frac{n}{2}} (1 - \alpha_{2i-1})$. To find the normalization explicitly, we know from Theorem 4.4 and Lemma 6.6 that $P(z, w)$ is up to normalization equal to $\det(zI + \Pi(w)) = z^2 + \text{tr } \Pi(w)z + \det \Pi(w)$, which is equal to

$$z^2 + z \frac{\alpha_{\text{odd}}}{\prod_{i=1}^{\frac{n}{2}} ((1 - \alpha_{2i-1})w - 1)} \text{tr} \prod_{i=1}^{\frac{n}{2}} \begin{bmatrix} u_{2i-1}(u_{2i} + (1 - \alpha_{2i})w) & u_{2i-1}(1 + u_{2i}) \\ (1 - \alpha_{2i})w + u_{2i}(1 - \alpha_{2i-1})w & 1 + u_{2i}(1 - \alpha_{2i-1})w \end{bmatrix} +$$

$$\frac{\alpha_{\text{odd}}}{\prod_{i=1}^{\frac{n}{2}} ((1 - \alpha_{2i-1})w - 1)} \alpha_{\text{odd}} u_{[n]} \prod_{i=1}^{\frac{n}{2}} ((1 - \alpha_{2i})w - 1),$$

which is

$$\frac{\alpha_{\text{odd}}}{\prod_{i=1}^{\frac{n}{2}} ((1 - \alpha_{2i-1})w - 1)} \left(\left(\frac{1}{\alpha_{\text{odd}}} \prod_{i=1}^{\frac{n}{2}} (1 - \alpha_{2i-1}) \right) z^2 w^{\frac{n}{2}} + \text{lower degree terms} \right).$$

Let $H_{(1,k)}$ denote the coefficient of zw^k in $P(z, w)$ for $k = 0, \dots, \frac{n}{2}$, so that when $k \in \{1, 2, \dots, \frac{n}{2} - 1\}$, they are the Hamiltonians of the dimer integrable system. Then we have

$$\sum_{k=0}^{\frac{n}{2}} H_{(1,k)} w^k = \frac{\prod_{i=1}^{\frac{n}{2}} ((1 - \alpha_{2i-1})w - 1)}{\alpha_{\text{odd}}} \text{tr } \Pi(w)$$

$$= \text{tr} \prod_{i=1}^{\frac{n}{2}} \begin{bmatrix} u_{2i-1}(u_{2i} + (1 - \alpha_{2i})w) & u_{2i-1}(1 + u_{2i}) \\ (1 - \alpha_{2i})w + u_{2i}(1 - \alpha_{2i-1})w & 1 + u_{2i}(1 - \alpha_{2i-1})w \end{bmatrix}.$$

Make the substitution $\beta_i = 1 - \alpha_i$ and consider the above expression as a polynomial in $\beta_1, \beta_2, \dots, \beta_n$. Since each $(1 - \alpha_i)$ inside the matrices appears with a w , the homogeneous component of degree k in $\beta_1, \beta_2, \dots, \beta_n$ is $H_{(1,k)} w^k$.

The main result of this section is the following simple procedure for converting between the AFIT Hamiltonians [AFIT20] and the dimer Hamiltonians.

Theorem 6.7. *The homogeneous degree k component of $\sum_{k=0}^{\frac{n}{2}} H_{(1,k)}$ as a polynomial in the variables $\alpha_1, \alpha_2, \dots, \alpha_n$ is, up to a sign, equal to $\sqrt{Y_{[n]} \alpha_{[n]}} \pi_{\vec{\alpha}}^* \circ \Lambda_{\vec{\alpha}}^* \left(\frac{F_k(c)}{\sqrt{e_{[n]}}} \right)$. For $k \in \{1, 2, \dots, \frac{n}{2} - 1\}$, these are AFIT Hamiltonians since $\sqrt{Y_{[n]} \alpha_{[n]}}$ is a Casimir. The homogeneous degree k component of $\sum_{k=0}^{\frac{n}{2}} H_{(1,k)}$ as a polynomial in $1 - \alpha_1, 1 - \alpha_2, \dots, 1 - \alpha_n$ is the dimer Hamiltonian $H_{(1,k)}$.*

Proof. By Corollary 6.5, $\Pi(1)$ is conjugated to $\pi_{\vec{\alpha}}^* \circ \Lambda_{\vec{\alpha}}^* M$ in PGL_2 . Since $\frac{1}{\det M} \text{tr}^2 M$ is a PGL_2 -conjugacy invariant, we have

$$\pi_{\vec{\alpha}}^* \circ \Lambda_{\vec{\alpha}}^* \left(\frac{1}{\sqrt{\det M}} \text{tr} M \right) = \pm \frac{1}{\sqrt{\det(\Pi(1))}} \text{tr}(\Pi(1)).$$

Using Theorem 2.3 and (30), we get

$$\sqrt{Y_{[n]}\alpha_{[n]}} \sum_{k=0}^{\frac{n}{2}} (-1)^k \pi_{\vec{\alpha}}^* \circ \Lambda_{\vec{\alpha}}^* \left(\frac{F_k(c)}{\sqrt{c_{[n]}}} \right) = \pm \sum_{k=0}^{\frac{n}{2}} H_{(1,k)}.$$

Note that the left side is a polynomial in α_i since $\pi_{\vec{\alpha}}^* \circ \Lambda_{\vec{\alpha}}^* \sqrt{c_{[n]}}$ has a factor $\sqrt{\alpha_{[n]}}$ which cancels the same factor in the numerator. Then the homogeneous component of degree k in the variables $\alpha_1, \alpha_2, \dots, \alpha_n$ on the left is $(-1)^k \sqrt{Y_{[n]}\alpha_{[n]}} \pi_{\vec{\alpha}}^* \circ \Lambda_{\vec{\alpha}}^* \left(\frac{F_k(c)}{\sqrt{c_{[n]}}} \right)$. \square

7 Odd n

For n odd, let Γ_n be obtained by gluing the graphs $G_1 G_2 \cdots G_{\frac{n-3}{2}} G_{\frac{n-1}{2}} G_n^{\text{odd}}$ from left to right and identifying w_{2n+1} with w_1 and w_{2n+2} with w_2 . The Newton polygon of Γ_n is (see Figure 3)

$$\text{Convex-hull} \left\{ (0, 0), (2, 0), \left(0, \frac{n-1}{2} \right), \left(2, \frac{n+1}{2} \right) \right\}.$$

We label the zig-zag paths as follows:

$$\begin{aligned} \xi_1 &= w_1, b_1, w_3, b_3, \dots, w_{2n-1}, b_{2n}, w_1, & [\xi_1] &= (1, 0), \\ \xi_2 &= w_2, b_2, w_4, b_4, \dots, w_{2n}, b_{2n-1}, w_2, & [\xi_2] &= (1, 0), \\ \sigma &= w_1, b_{2n-1}, w_{2n}, b_{2n-2}, \dots, w_4, b_1, w_1, & [\sigma] &= (-2, -1), \\ \zeta_{2i-1} &= w_{4i-1}, b_{4i-3}, w_{4i}, b_{4i-2}, w_{4i-1}, & [\zeta_{2i-1}] &= (0, 1), \\ \zeta_{2i} &= w_{4i-1}, b_{4i}, w_{4i}, b_{4i-1}, w_{4i-1}, & [\zeta_{2i}] &= (0, -1), \\ \zeta_n &= w_{2n+1}, b_{2n}, w_{2n+2}, b_{2n-1}, & [\zeta_{2i-1}] &= (0, 1), \end{aligned}$$

where $i \in \{1, 2, \dots, \frac{n-1}{2}\}$.

Let N denote the Newton polygon of Γ_n . We define a rational map $\pi_{\vec{\alpha}} : \mathcal{X}_{N, \vec{\alpha}} \supset \mathcal{L}_{\Gamma_n, \vec{\alpha}} \rightarrow (\mathbb{C} \setminus \{0, -1\})^n$:

$$\pi_{\vec{\alpha}}^* u_i = Y_i, \tag{31}$$

for all $i \in \{1, 2, \dots, n\}$, which is checked to be Poisson as in the even case. We have

$$\begin{aligned} \Pi_{G_n^{\text{odd}}}(w) &= \frac{\alpha_n}{(1 - \alpha_n)w - 1} \begin{bmatrix} 1 & (1 - \alpha_n)w \\ u_n & u_n \end{bmatrix}, \\ \det \Pi_{G_n^{\text{odd}}}(w) &= \frac{\alpha_n}{(1 - \alpha_n)w - 1} (-\alpha_n u_n), \\ \det \Pi_{G_n^{\text{odd}}}(1) &= \alpha_n u_n. \end{aligned} \tag{32}$$

Let $\Pi(w)$ denote the monodromy matrix of Γ_n . As in the even case, we have $\det \Pi(1) = \alpha_{[n]} u_{[n]}$. Let $P(z, w)$ denote the characteristic polynomial of Γ_n normalized as follows

$$\det(zI + \Pi(w)) = \frac{\alpha_{\text{odd}}}{\prod_{i \text{ odd}} ((1 - \alpha_{2i})w - 1)} P(z, w).$$

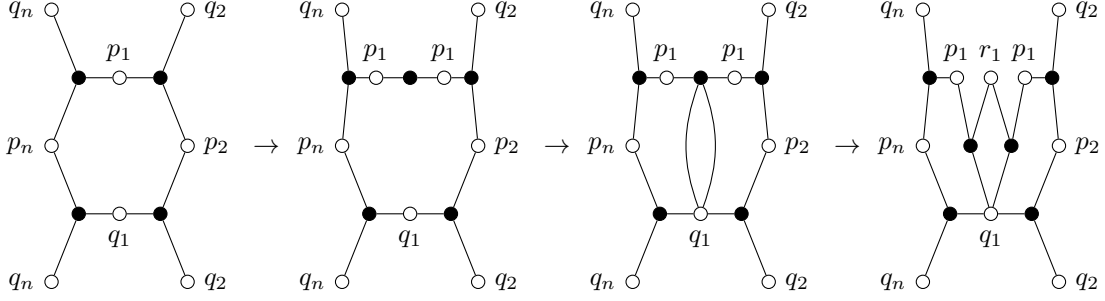


Figure 9: Insertion of r_1 in the fundamental domain.

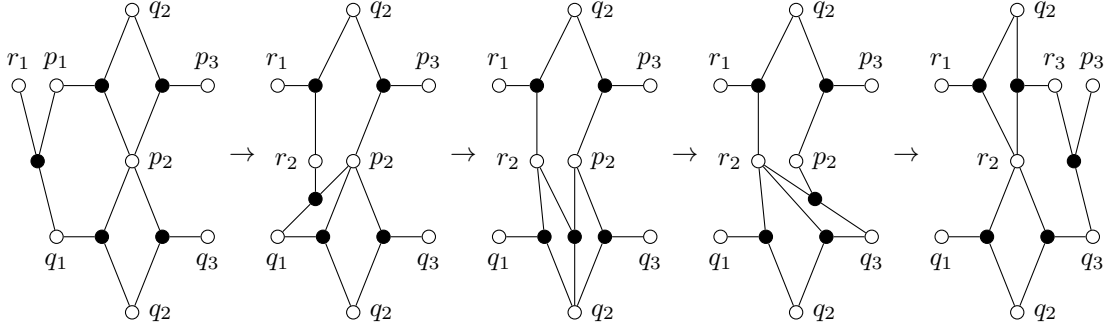


Figure 10: Beginning of the sequence of local moves that propagates r through (p, q) .

Let $H_{(1,k)}$ denote the coefficient of zw^k in $P(z, w)$ for $k = 1, \dots, \frac{n+1}{2}$. Note that $(1 - \alpha_n)$ appears with a w in (32), so as before $H_{(1,k)}w^k$ is the homogeneous component of degree k in $1 - \alpha_1, 1 - \alpha_2, \dots, 1 - \alpha_n$. Theorem 6.7 holds verbatim, after making the necessary adjustment of the indices.

Theorem 7.1. *The homogeneous degree k component of $\sum_{k=0}^{\frac{n}{2}} H_{(1,k)}$ as a polynomial in the variables $\alpha_1, \alpha_2, \dots, \alpha_n$ is, up to a sign, equal to $\sqrt{Y_{[n]}\alpha_{[n]}}\pi_{\vec{\alpha}}^* \circ \Lambda_{\vec{\alpha}}^* \left(\frac{F_k(c)}{\sqrt{c_{[n]}}} \right)$. For $k \in \{1, 2, \dots, \frac{n-1}{2}\}$, these are AFIT Hamiltonians since $\sqrt{Y_{[n]}\alpha_{[n]}}$ is a Casimir. The homogeneous degree k component of $\sum_{k=0}^{\frac{n}{2}} H_{(1,k)}$ as a polynomial in $1 - \alpha_1, 1 - \alpha_2, \dots, 1 - \alpha_n$ is the dimer Hamiltonian $H_{(1,k)}$.*

8 Cross-ratio dynamics via local moves

In this section we show that cross-ratio dynamics, that is the map $\nu_{\vec{\alpha}} : (p, q, M) \mapsto (q, r, M)$ is identified with a certain sequence of local moves on the dimer side. We prepare with an observation on multi-ratios.

Lemma 8.1. *Assume p, q, r are nondegenerate twisted curves such that $p \neq r$ and both p and r are $\vec{\alpha}$ -related to q . Then*

$$\text{mr}(p_i, q_i, r_i, r_{i+1}, q_{i+1}, p_{i+1}) = -1 \quad (33)$$

holds for all $i \in \mathbb{Z}$.

Proof. The Lemma follows directly from the fact that both

$$\text{cr}(p_i, q_i, q_{i+1}, p_{i+1}) = \text{cr}(q_i, r_i, r_{i+1}, q_{i+1}), \quad (34)$$

$$\text{mr}(p_i, q_i, r_i, r_{i+1}, q_{i+1}, p_{i+1}) = -\frac{\text{cr}(p_i, q_i, q_{i+1}, p_{i+1})}{\text{cr}(q_i, r_i, r_{i+1}, q_{i+1})} \quad (35)$$

hold for all $i \in \mathbb{Z}$. □

Now we construct the sequence of moves.

Theorem 8.2. *Suppose $[\text{wt}] \in \mathcal{X}_{N, \bar{\alpha}}$ is such that $u^{-1} \circ \pi_{\bar{\alpha}}([\text{wt}]) = (p, q, M)$. Consider the sequence of moves shown in Figures 9, 10, and let μ denote the induced birational map of weights. Then the pair of curves (q, r, M) is $u^{-1} \circ \pi_{\bar{\alpha}} \circ \mu([\text{wt}])$. In other words, the following diagram commutes:*

$$\begin{array}{ccc} \mathcal{X}_{N, \bar{\alpha}} & \xrightarrow{u^{-1} \circ \pi_{\bar{\alpha}}} & \mathcal{U}_n \\ \downarrow \mu & & \downarrow \nu_{\bar{\alpha}} \\ \mathcal{X}_{N, \bar{\alpha}} & \xrightarrow{u^{-1} \circ \pi_{\bar{\alpha}}} & \mathcal{U}_n \end{array}$$

Proof. By Lemma 6.4, it suffices to trace what happens to the TCD map associated to $[\text{wt}]$ through the sequence of moves. Let us initially assume that we deal with a periodic instead of a twisted curve. Assume n is even. We proceed in four steps:

1. First, we need to insert r_1 into the graph, see Figure 9 for an illustration. To do this, we begin by splitting p_1 into two copies of p_1 and a new black vertex b . Then we add a bigon with vertices b, q_1 , such that the bigon is inside the face also bounded by p_2 and p_n . Finally we split b into two new black vertices of degree three while also generating the new white vertex corresponding to r_1 .
2. We apply a sequence of spider moves and resplits to propagate r_1 through the graph, see Figure 10. To replace both p_{2i-1} and p_{2i} with r_{2i} and r_{2i+1} we need to apply a resplit, then two spider moves and then a resplit again. Each time we apply a resplit, we check that the points before and after are related as in Lemma 8.1. This ensures that we are not changing the face-weights of Γ , as discussed in Section 5.1. We apply these moves until we have replaced p_n with a new copy of r_1 .
3. After the moves of step 2, there is still one copy of p_1 left in the graph. The situation at p_1 looks like in the rightmost graph in Figure 9, except that the roles of p and r are interchanged. We can therefore absorb p_1 again by doing step 1 backwards. Here, it is essential that the two copies of r_1 coincide with each other in \mathbb{CP}^1 . After a rescaling at r_1 , we can assume the lifts in \mathbb{C}^2 coincide as well. This ensures that the corresponding edge-weights in the contraction and the removal of the bigon agree up to a common factor. This common factor can be set to -1 by a rescaling at one of the involved black vertices.
4. Finally, we translate Γ_n by $\frac{1}{2}\gamma_w$ to interchange q and r .

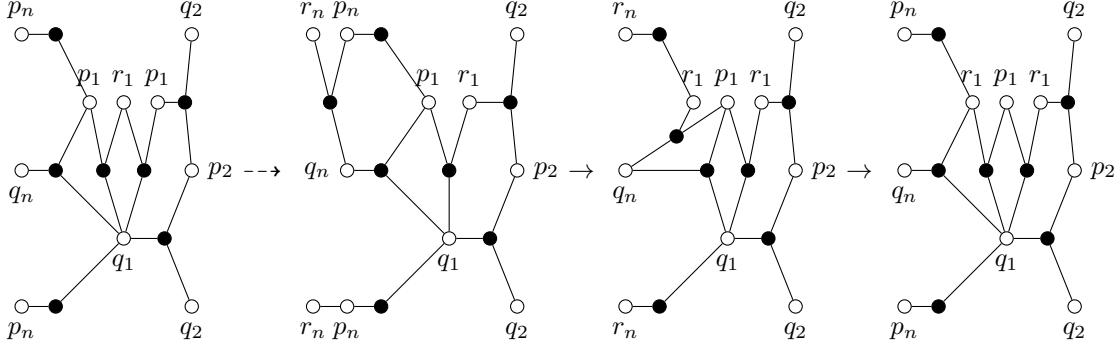


Figure 11: Key steps in cross-ratio dynamics via local moves for n odd.

If n is not even, the procedure is almost identical. We also split p_1 , but we insert the bigon in the face also bounded by p_2 and q_n . Propagation and absorption of p_1 works as in the even case, see Figure 11 for an illustration. This concludes the proof in the periodic case. In the twisted case, we apply the same sequence of moves in the fundamental domain. Instead of inserting r_1 , we simultaneously insert $r_{1+m\gamma_z}$ for all $m \in \mathbb{Z}$. We proceed analogously in Step 3, where we contract pairs of $p_{1+m\gamma_z}$ for all $m \in \mathbb{Z}$. \square

Since the weights of the two edges of a bigon sum to zero, the weight of any dimer cover that uses one of the edges of the bigon is canceled by the weight of the dimer cover that uses the other edge. Therefore the dimer Hamiltonians are unchanged on inserting a bigon. Since the dimer Hamiltonians are also preserved by the elementary transformations ([GK13, Theorem 4.7]), we obtain:

Corollary 8.3. *The dimer Hamiltonians are invariant under cross-ratio dynamics.*

Acknowledgements

TG thanks Nick Ovenhouse for discussions about networks in a cylinder. SR thanks Ivan Izmetiev for discussions on cross-ratio dynamics during a visit at TU Wien. NA was supported by the Deutsche Forschungsgemeinschaft (DFG) Collaborative Research Center TRR 109 “Discretization in Geometry and Dynamics”. SR is partially supported by the Agence Nationale de la Recherche, Grant Number ANR-18-CE40-0033 (ANR DIMERS) and by the CNRS grant Tremplin@INP.

Appendix A Schur complement

Suppose $M = \begin{bmatrix} A & B \\ C & D \end{bmatrix}$ is a $(p+q) \times (r+q)$ block matrix with D an invertible $q \times q$ matrix. Let $V := \text{coker } M$. Let e_i denote the i th basis column vector, and let $v_i \in V$ denote the image of e_i under the cokernel map. Let $M/D := A - BD^{-1}C$ denote the Schur complement.

Theorem A.1 (Schur determinant formula [Sch17]). *If M is a square matrix ($p = r$), then we have*

$$\det(M) = \det(D)\det(M/D).$$

Theorem A.2. *coker $M/D \cong \text{coker } M$, and under this identification the cokernel map of M/D is $e_i \mapsto v_i$ for $i = 1, \dots, p$.*

Proof. After a change of basis, M takes the block diagonal form $\begin{bmatrix} M/D & 0 \\ 0 & D \end{bmatrix}$:

$$M = \begin{bmatrix} I & BD^{-1} \\ 0 & I \end{bmatrix} \begin{bmatrix} M/D & 0 \\ 0 & D \end{bmatrix} \begin{bmatrix} I & 0 \\ D^{-1}C & I \end{bmatrix}.$$

Since D is invertible, we have $\text{coker } D = 0$. Therefore we have $\text{coker } M \cong \text{coker } M/D \oplus \text{coker } D \cong \text{coker } M/D$. Under the change of basis $\begin{bmatrix} I & BD^{-1} \\ 0 & I \end{bmatrix}$ of \mathbb{C}^{p+q} , we have

$$e_i \mapsto \begin{bmatrix} I & BD^{-1} \\ 0 & I \end{bmatrix}^{-1} e_i = e_i \text{ for } i = 1, 2, \dots, p,$$

from which we see that the cokernel map of M/D , when we identify $\text{coker } M/D$ with $\text{coker } M = V$, is given by $e_i \mapsto v_i$. \square

References

- [AFIT20] Maxim Arnold, Dmitry Fuchs, Ivan Izmistiev, and Serge Tabachnikov, *Cross-ratio dynamics on ideal polygons*, Int. Math. Res. Not. IMRN (2020). Published online.
- [AGPR19] Niklas Affolter, Max Glick, Pavlo Pylyavskyy, and Sanjay Ramassamy, *Vector-relation configurations and plabic graphs*, arXiv preprint arXiv:1908.06959 (2019).
- [AGR] Niklas Affolter, Max Glick, and Sanjay Ramassamy, *Triple crossing diagram maps and multiple cluster structures*. In preparation.
- [BP96] Alexander Bobenko and Ulrich Pinkall, *Discrete isothermic surfaces*, J. Reine Angew. Math. **475** (1996), 187–208. MR1396732
- [Che20] Sunita Chepuri, *Plabic R -matrices*, Publ. Res. Inst. Math. Sci. **56** (2020), no. 2, 281–351. MR4082905
- [CR08] David Cimasoni and Nicolai Reshetikhin, *Dimers on surface graphs and spin structures. II*, Comm. Math. Phys. **281** (2008), no. 2, 445–468. MR2410902
- [EFS12] Richard Eager, Sebastián Franco, and Kevin Schaeffer, *Dimer models and integrable systems*, J. High Energy Phys. **6** (2012), 106, front matter+24. MR3006855
- [FG09] Vladimir V. Fock and Alexander B. Goncharov, *Cluster ensembles, quantization and the dilogarithm*, Ann. Sci. Éc. Norm. Supér. (4) **42** (2009), no. 6, 865–930. MR2567745
- [FM16] Vladimir V. Fock and Andrey Marshakov, *Loop groups, clusters, dimers and integrable systems*, Geometry and quantization of moduli spaces, 2016, pp. 1–66. MR3675462
- [FZ02] Sergey Fomin and Andrei Zelevinsky, *Cluster algebras. I. Foundations*, J. Amer. Math. Soc. **15** (2002), no. 2, 497–529. MR1887642
- [GK13] Alexander B. Goncharov and Richard Kenyon, *Dimers and cluster integrable systems*, Ann. Sci. Éc. Norm. Supér. (4) **46** (2013), no. 5, 747–813. MR3185352
- [Gli11] Max Glick, *The pentagram map and Y -patterns*, Adv. Math. **227** (2011), no. 2, 1019–1045. MR2793031
- [GP16] Max Glick and Pavlo Pylyavskyy, *Y -meshes and generalized pentagram maps*, Proc. Lond. Math. Soc. (3) **112** (2016), no. 4, 753–797. MR3483131

- [GR17] Max Glick and Dylan Rupel, *Introduction to cluster algebras*, Symmetries and integrability of difference equations, 2017, pp. 325–357. MR3677355
- [GSTV16] Michael Gekhtman, Michael Shapiro, Serge Tabachnikov, and Alek Vainshtein, *Integrable cluster dynamics of directed networks and pentagram maps*, Adv. Math. **300** (2016), 390–450. MR3534837
- [GSV12] Michael Gekhtman, Michael Shapiro, and Alek Vainshtein, *Poisson geometry of directed networks in an annulus*, J. Eur. Math. Soc. (JEMS) **14** (2012), no. 2, 541–570. MR2881305
- [HJ03] Udo Hertrich-Jeromin, *Introduction to Möbius Differential Geometry*, London Mathematical Society Lecture Note Series, Cambridge University Press, 2003.
- [HJMNP01] U. Hertrich-Jeromin, I. McIntosh, P. Norman, and F. Pedit, *Periodic discrete conformal maps*, J. Reine Angew. Math. **534** (2001), 129–153. MR1831634
- [ILP16] Rei Inoue, Thomas Lam, and Pavlo Pylyavskyy, *Toric networks, geometric R-matrices and generalized discrete Toda lattices*, Comm. Math. Phys. **347** (2016), no. 3, 799–855. MR3551255
- [ILP19] ———, *On the cluster nature and quantization of geometric R-matrices*, Publ. Res. Inst. Math. Sci. **55** (2019), no. 1, 25–78. MR3898323
- [Izo21] Anton Izosimov, *Dimers, networks, and cluster integrable systems*, arXiv preprint arXiv:2108.04975 (2021).
- [Kas63] P. W. Kasteleyn, *Dimer statistics and phase transitions*, J. Math. Phys. **4** (1963), 287–293. MR153427
- [NC95] Frank Nijhoff and Hans Capel, *The discrete Korteweg-de Vries equation*, 1995, pp. 133–158. KdV '95 (Amsterdam, 1995). MR1329559
- [OST10] Valentin Ovsienko, Richard Schwartz, and Serge Tabachnikov, *The pentagram map: a discrete integrable system*, Comm. Math. Phys. **299** (2010), no. 2, 409–446. MR2679816
- [OST13] Valentin Ovsienko, Richard Evan Schwartz, and Serge Tabachnikov, *Liouville-Arnold integrability of the pentagram map on closed polygons*, Duke Math. J. **162** (2013), no. 12, 2149–2196. MR3102478
- [Sch17] J. Schur, *Über Potenzreihen, die im Innern des Einheitskreises beschränkt sind*, J. Reine Angew. Math. **147** (1917), 205–232. MR1580948
- [Sol13] Fedor Soloviev, *Integrability of the pentagram map*, Duke Math. J. **162** (2013), no. 15, 2815–2853. MR3161305

TECHNISCHE UNIVERSITÄT BERLIN, INSTITUTE OF MATHEMATICS, STRASSE DES 17. JUNI 136, 10623 BERLIN, GERMANY

E-mail address: `affolter at math.tu-berlin.de`

UNIVERSITY OF MICHIGAN, DEPARTMENT OF MATHEMATICS, 2844 EAST HALL, 530 CHURCH STREET, ANN ARBOR, MI 48109-1043, USA

E-mail address: `georgete at umich.edu`

UNIVERSITÉ PARIS-SACLAY, CNRS, CEA, INSTITUT DE PHYSIQUE THÉORIQUE, 91191 GIF-SUR-YVETTE, FRANCE

E-mail address: `sanjay.ramassamy at ipht.fr`